STATUS REPORTS

to the

PAPER PHYSICS

PROJECT ADVISORY COMMITTEE

Volume I

March 24, 1998

INSTITUTE OF PAPER SCIENCE AND TECHNOLOGY

Atlanta, Georgia

ANNUAL RESEARCH REVIEW

PAPER PHYSICS

VOLUME I

MARCH 24, 1998

February 18, 1998

TO: MEMBERS OF THE PAPER PHYSICS PROJECT ADVISORY COMMITTEE

Attached for your review are the Status Reports for the projects to be discussed at the Paper Physics Project Advisory Committee meeting. The Program Review is scheduled for Tuesday, March 24, 1998, at 8:00 a.m. - 12:00 p.m. and the PAC Committee Meeting will be held from 1:00 p.m. to 5:00 p.m.

Please note that the meeting is being held at the Institute of Paper Science and Technology.

We look forward to seeing you at this time.

Sincerely,

John Waterhouse
Acting Director
Fiber and Paper Physics Division

JFW/djh

Attachment

Institute of Paper Science and Technology, Inc.

500 10th Street, N.W.
Atlanta, GA 30318-5794

Telephone 404-894-570
FAX# 404-894-IPST (4778

PAPER PHYSICS
PROJECT ADVISORY COMMITTEE

IPST Liaison: Mr. John Waterhouse (404) 894-5756; FAX (404) 894-4778
RAC Liaison: Dr. Walter Freeman (302) 995-3249; FAX (302) 995-3794
Alternate: Dr. John Goss (408) 255-1500; FAX (408) 864-7551

Dr. Keith A. Bennett *(2000)
Senior Research Scientist
Weyerhaeuser Company
WTC 2B22
Tacoma, WA 98477-0001
(206) 924-6714
(206) 924-6324 FAX

Dr. Doeung Choi *(2001)
Senior Research Engineer
Hercules Incorporated
Paper Technology Division
500 Hercules Road
Wilmington, DE 19808-1599
(302) 995-3650
(302) 995-4565 FAX

Mr. Anthony R. Colasurdo *(2001)
Technical Manager
EKA Chemicals Inc.
211 Newmarket Parkway
Suite 106
Marietta, GA 30067
(770) 956-2520
(770) 984-1260 FAX

Mr. Timothy Hess *(1998)
Chemist/Engineer
P.H. Glatfelter Co.
228 South Main Street
Spring Grove, PA 17362-1000
(717) 225-4711 x2626
(717) 225-7394 FAX
thess@glatfelter.com

Dr. Patricia N. Hurter *(2001)
Group Leader
Union Camp Corporation
Post Office Box 3301
Princeton, NJ 08543-3301
(609) 844-7273
(609) 844-7323 FAX

Mr. Mont A. Johnson *(2001)
Senior Physicist
Honeywell-Measurex
MS 1122
One Results Way
Cupertino, CA 95014
(408) 255-1500
johnson.mont@measurex.com

Dr. David E. Knox *(2001)
Research Group Leader
Westvaco Corporation
Kraft Division
5600 Virginia Avenue
North Charleston, SC 29411
(803) 745-3982

Dr. Leslie L. Martin *(1998)
Manager, Papermaking R&D
Potlatch Corporation
Fiber R&D - Post Office Box 503
East End Avenue E
Cloquet, MN 55720-0503
(218) 879-2387
(218) 879-2375 FAX

Dr. Robert J. Niebauer *(2001)
Manager, R&D, Raw Materials, and ISO Department
Crane & Co., Inc.
30 South Street
Dalton, MA 01226-1751
(413) 684-2600
(413) 684-1789 FAX

Ms. Jennice L. Ozment *(Alternate)
Applications Scientist
EKA Chemicals Inc.
2211 Newmarket Parkway
Suite 106
Marietta, GA 30067
(770) 956-2520

Mr. Jeffrey R. Reese *(Alternate)
Consultant, Paper Mill
Georgia-Pacific Corporation
133 Peachtree Street, NE
18th Floor
Atlanta, GA 30303
(404) 652-4880
(404) 584-1466 FAX
JReese@GAPAC.com

Mr. Thomas E. Rodencal *(2001)
Sr. Paper Mill Staff Engineer
Georgia-Pacific Corporation
133 Peachtree Street, NE
18th Floor
Atlanta, GA 30303
(404) 652-4514
(404) 584-1466 FAX

* The dates in ( ) indicate the final year of the appointment.

Paper Physics PAC (cont.)

Mr. Arvind Sahay *(1999)
Director, Product Development
Asten, Inc.
213 Boulevard Du Harve
Valleyfield, Quebec CANADA J6S 1R9
(514) 373-2424
(514) 373-4745 FAX

Dr. Jack Schulz *(1998)
Portfolio Manager - Product Development
Champion International Corporation
West Nyack Road
West Nyack, NY 10994
(914) 578-7000
(914) 578-7175 FAX

Mr. Dan H. Sze *(2001)
Manager, Paper Technology
Beloit Corporation
Rockton Research Center
1165 Prairie Hill Road
Rockton, IL 61072-1595
(608) 364-8525
(608) 364-8600 FAX
dhsze@beloit.com

Ms. Meredith M. Schoppee *(2000)
Research Associate
Albany International Corporation
Textile Physics Group
777 West Street
Mansfield, MA 02048-9114
(508) 337-9578
(508) 339-4996 FAX
meredith_schoppee@albint.com

Mr. Dirk E. Swinehart *(1998) (Chairman)
Fellow, Paper Physics
Fiber Development
Mead Central Research
8th and Hickory Streets
Chillicothe, OH 45601-5700
(614) 772-3570
(614) 772-3595 FAX
DESI@mead.com

Dr. Gary L. Worry *(1998)
Manager, Core Technology
Fort James Corporation
1915 Marathon Avenue
Post Office Box 899
Neenah, WI 54957-0899
(414) 729-8470
(414) 729-8144 FAX

* The dates in ( ) indicate the final year of the appointment.

PAPER PHYSICS
PROJECT ADVISORY COMMITTEE MEETING

MARCH 24, 1998

Institute of Paper Science and Technology
Atlanta, Georgia

PROGRAM REVIEW AGENDA

Room 114

8:00 a.m. - 8:10 a.m.	Opening Remarks and Antitrust Statement	John Waterhouse & Dirk Swinehart
8:10 a.m. - 8:20 a.m.	Welcome from Vice President of Research	Gary Baum
8:20 a.m. - 8:50 a.m.	Project F007 On-line Measurement of Paper Properties	Mac Hall
8:50 a.m. - 9:20 a.m.	Project F008 Fundamentals of Acoustic Radiation	Pierre Brodeur
9:20 a.m. - 9:50 a.m.	Project F020 Fundamentals of Dimensional Stability	Doug Coffin
9:50 a.m. - 10:00 a.m.	Break	
10:00 a.m. - 10:30 a.m.	Project F026 Fundamentals of Accelerated Creep	Chuck Habeger
10:30 a.m. - 11:00 a.m.	Project F023 Micromechanics of Fiber Networks	Martin Ostaja
11:00 a.m. - 11:30 a.m.	Project F024 Fundamentals of Refining and Fiber Properties	John Waterhouse
11:30 a.m. - 12:00 a.m.	Project F025 Fundamentals of Interfiber Bonding	Hiroki Nanko

Room 173

1:00 p.m. - 5:00 p.m.	Paper Physics Committee Discussions

PAPER PHYSICS
PROJECT ADVISORY COMMITTEE MEETING

MARCH 24, 1998

Institute of Paper Science and Technology
Atlanta, Georgia

COMMITTEE AGENDA

Room 173

1:00 p.m. – 1:15 p.m.

- Antitrust/Confidentiality Statements
- Next Meeting Date
- Review Agenda

1:15 p.m. – 2:00 p.m.

- RAC Liason's Overview of Research Lines/Roadmaps
- Research Lines/Roadmaps
- Research Ideas List
- Project Review Critique Forms

2:00 p.m. – 3:30 p.m.

- Subcommittee Project Reviews
  - F007 On-line Measurement of Paper Properties
  - F008 Fundamentals of Acoustic Radiation Pressure
  - F020 Fundamentals of Dimensional Stability
  - F026 Fundamentals of Accelerated Creep
  - F023 Micromechanics of Fiber Networks
  - F024 Fundamentals of Refining and Fiber Properties
  - F025 Fundamentals of Bonding

3:30 p.m. – 5:00 p.m.

- Full Committee Project Reviews and Summaries
- Close Meeting

TABLE OF CONTENTS

Volume I

Volume II

ON-LINE MEASUREMENT OF PAPER PROPERTIES

STATUS REPORT

FOR

PROJECT F007

Mac Hall
Ted Jackson
Andy Brown

Institute of Paper Science and Technology
500 10th Street, N. W.
Atlanta, Georgia 30318

DUES-FUNDED PROJECT SUMMARY

Project Title: ON-LINE MEASUREMENT OF PAPER PROPERTIES
Project Code: ONLIN
Project Number: F007
PAC: Paper Physics
Division: Fiber and Paper Physics
Project Staff: Mac Hall, Ted Jackson, Andy Brown
FY 97-98 Budget: $85,012
Allocated as Cost Share in Cooperative Agreement No. DE-FC02-95CDE41156
Time Allocation: 20%
Supporting Research
Related External Funding for FY 97-98: DOE/OIT - $599,900

RESEARCH LINE/ROADMAP

10. Energy Performance
12. Sensors and Process Control

PROJECT OBJECTIVE

This project is focused on the fundamentals of paper stiffness measurement using ultrasonics and the relationships of ZD and in-plane stiffnesses to on-machine process parameters. It supplements the project to develop commercially viable sensors and instrumentation capable of measuring the velocity of ultrasound in the in-plane and thickness directions of the paper web as it is being made on the paper machine.

PROJECT BACKGROUND

The variations of the elastic stiffnesses of paper with refining, fiber orientation, wet pressing pressure, wet straining (draws), and drying restraints have been studied and reported (Baum et al., 1984; Habeger and Baum, 1986). These studies have demonstrated that elastic stiffnesses are sensitive to changes in furnish and to changes in the various process parameters. Measurement on the paper machine of the elastic stiffnesses in both the in-plane and thickness directions along with the basis weight, moisture, and caliper of the web should provide means to continuously monitor product quality and data to control the paper manufacturing process.

The instrumentation should be applicable to most grades of paper, but will be particularly beneficial to the heavier weight grades, packaging paper and paperboard, because "strength" properties are of primary importance for these products. Energy waste is avoided by minimizing the amount of substandard production, particularly during grade changes, which must be repulped and remanufactured. Further energy savings should result from optimum utilization of refining and drying (Lantz and Chase, 1988), and from efficiency improvement in subsequent converting processes as a result of product uniformity.

A 1000-ton/day machine producing 350,000 tons/year uses approximately 4.725 trillion Btu/year. For each 1% of production that is substandard and reprocessed at 13.5 million Btu/ton, the 1000-ton/day machine wastes 47.25 billion Btu/year. Substandard production may be as high as 5 percent. Assuming this technology will reduce substandard production by 2% (i.e., to 3% rather than 5%), the energy saving would be 94.5 billion Btu/year or $378,000 (@ $4/million Btu) annually for the 1000-ton/day machine.

Refining requires approximately 200 kWh/ton or 2.1 million Btu/ton (1 kWh = 10,500 Btu). For a 1000-ton/day machine, the annual energy usage for refining is approximately 70.0 million kWh or 735 billion Btu. Assuming the optimization of refining could reduce the energy required by 10%, this would be equivalent to a savings of 73.5 billion Btu or $294,000 annually.

By decreasing refining, drainage is improved, requiring less steam for drying the web. The steam required for drying is equivalent to approximately 8 million Btu/ton, or 2.8 trillion Btu/year for a 1000-ton/day machine. If the moisture of the paper entering the dryer is reduced by 1.0%, the dryer steam required would be reduced by about 3%. This would save an additional 84 billion Btu/year or $336,000 annually.

Summary for a 1000-ton/day paper machine:

Annual Energy Use = 4.725 trillion Btu = $18,900,000 @ $4/million Btu

Reprocessing savings:

*	Electricity	38.5 billion Btu	
*	Steam	56.0 billion Btu	
	Total reprocessing savings	94.5 billion Btu	= $378,000

Refining savings:

*	Electricity	73.5 billion Btu	= $294,000

Drying savings:

*	Steam	84.0 billion Btu	= $336,000

Total potential savings for 1000-ton/day machine:

*	Electricity	112.0 billion Btu	= $448,000
*	Steam	140.0 billion Btu	= $560,000
		@ $4/million Btu	= $1,008,000
	Total savings/year	252 billion Btu/year	= 5.3%

Additional benefits of the technology are difficult to quantify. The ability to control to stiffness targets not only minimizes energy waste, but also provides the potential environmental benefit of using fewer trees. The paper manufacturer would be able to monitor the effect of recycled fiber utilization on product quality and thus could use higher percentages of recycled fiber with confidence that the product remains within specifications.

Minimizing the need to repulp and remanufacture reduces water utilization and provides consequential benefits to the environment. An additional waste that is difficult to quantify is the "waste" of fiber quality that occurs each time the fibers are dried and rewet. This type of waste is avoided by making quality paper the first time through the paper machine.

While designing and developing instrumentation to demonstrate on-machine measurement in a mill, this project has supported various related studies in the

laboratory. These studies provide background and support for verifying on-machine sensor performance and on-machine measurement and process relationships.

Some examples are:

Demonstrated repeatable measurements of short-range variations of MD, CD, and ZD ultrasonic velocities for cross-machine samples of machine-made papers.

Ultrasonic velocity measurements of CD strips show large short-range variations that appear similar to the nonuniformities, streaks, and "dry-line fingers" observed on the forming table.

Examined various correlation techniques to determine relationships between ultrasonic velocity measurements and compressive strength measurements, Ring Crush (RC) and short-span compressive strength (STFI).

Developed system to make high resolution measurements of basis weight (using the ABB Beta gauge) and ultrasound velocity in the ZD (using fluid-filled wheels) for paper samples mounted on the laboratory web handler.

Demonstrated sensitivity of ZD ultrasonic measurements to wet pressing and calendering using samples made on Herty pilot machine.

SUMMARY OF RESULTS (March 97 - March 98)

IPST Technical Paper Series Number 641: "Small-Scale Variations in CD Strips Observed Using Ultrasonic Velocity Measurements," by M. S. Hall and T. G. Jackson. Presented at International CD Symposium, Tampere, Finland, June 5, 1997.

IPST Technical Paper Series Number 665: "New On-Line Out-of-Plane Ultrasonic Elastic Stiffness Measurement Technology," by T. Jackson and M. Hall. Presented at 1997 TAPPI Process and Product Quality Conference, October 2, 1997.

Applied multivariable statistical analysis to data for samples from Herty pilot machine run, April 1-4, 1997.

Tape-pull examples suggest short range structural formation in some papers that may be observed with high resolution ultrasonic measurements.

PROJECT GOALS FOR FY 98-99

Fundamental study of relationships between elastic constants and properties that may be inferred from online ultrasonic measurements (C. Habeger and D. Coffin).

[See appended discussion of "Relationships between Elastic Constants" by C. Habeger]

Verify on-machine ultrasonic sensor measurements by comparison with laboratory instrument measurements.

Determine relationships between on-machine ultrasonic velocity measurements and papermaking process variables, e.g., refining, wet pressing, wet straining, and calendering. Emphasize the sensitivity of ZD ultrasonic measurements to process variables.

Compare "structural" formation observable with ultrasonics to formation observed with "beta" measurements.

PROJECT DELIVERABLES:

Verification of on-machine sensor measurements.

Report on observed relationships between on-machine ultrasonic velocity measurements and papermaking process variables

PROJECT SCHEDULE:

	1998			1999			
	Apr-Jun	Jul-Sep	Oct-Dec	Jan-Mar	Apr-Jun	Jul-Sep	Oct-Dec
1. Elastic constants/ properties relationships (with student)	------	------	------	------	-----*		
2. Verify on-machine sensors: (1) In-plane; (2) ZD	------	-----1	------	-----2			
3. On-machine measurement/ process relationships		------	------	------	------	-----*	
4. Structural Formation ?		------	------	-----*			
5. Final Report					------	------	--*

OBSERVATIONS AND DISCUSSION

High Resolution Measurements

While developing and evaluating the measurement capability of our ultrasonic instrumentation in the laboratory, we have reported observing repeatable measurement of large short-range variations in the properties of typical machine-made papers. We have demonstrated the ability to make in-plane and ZD ultrasonic velocity measurements and basis weight measurements at intervals as small as 1 millimeter.

At a TAPIO Users Club meeting in Tampere, Finland, June 3, 1997, Mark Ryan of Mead Escanaba reported on observations related to "Finger Ridges." He reported using tape-pull methods to observe bands of machine direction oriented fibers on the wire side. These appear to be related to the tube spacing in the head box (Aidun, 1996). However, high resolution analysis of the basis weight and caliper of the uncoated paper showed no peaks at the tube spacing frequency.

We have experimented with a paper sample that shows bands of machine direction oriented fibers on the wire side using tape pulls. Using in-plane ultrasonic velocity measurements in the MD at 1-millimeter intervals, the results appear to correlate with the fiber orientation found with a subsequent tape pull. We hope to explore further the

possibility that in-plane and ZD ultrasonics may be used to characterize "structural formation" that may not be observed with high-resolution basis weight measurements.

In-Plane Ultrasonic Measurements

The on-machine in-plane sensor will measure the CD longitudinal velocity (V_{CD}) and the shear velocity (V_{SH}) in the cross direction. We are also interested in knowing the MD longitudinal velocity (V_{MD}). This can be calculated in the following way.

We start with the relationship (Baum, et al., 1981)

$$G = \rho(V_{SH})^2 = \frac{[(E_{MD})(E_{CD})]^{1/2}}{2[1 + (\nu_{MD}\nu_{CD})^{1/2}]} \quad (1)$$

For anisotropy ratios less than 3, the in-plane Poisson ratio, $(\nu_{MD}\nu_{CD})^{1/2}$, was found by Baum, et. al., to be essentially constant with a mean value of 0.293. Substituting this into Eqn. 1 gives

$$\rho(V_{SH})^2 = 0.387\ [(E_{MD})(E_{CD})]^{1/2} \quad (2)$$

where $E_{MD} = \rho(V_{MD})^2\ (1 - \nu_{MD}\nu_{CD})$ and $E_{CD} = \rho(V_{CD})^2\ (1 - \nu_{MD}\nu_{CD})$

I have substituted $(V_{MD})(V_{CD})$ for $[(E_{MD})(E_{CD})]^{1/2}$ in the past in this equation since the density cancels out of the equation and the Poisson ratio is small. However, the Poisson ratio should not be ignored in the relationship between E and V. Substituting these into Eqn. 2,

$$(V_{SH})^2 = 0.387\ (V_{MD})(V_{CD})\ (1 - \nu_{MD}\nu_{CD}),\ \text{where } \nu_{MD}\nu_{CD} = (0.293)^2 \quad (3)$$

or $$(V_{SH})^2 = 0.354\ (V_{MD})(V_{CD}) \quad (4)$$

Thus, it is only necessary to measure the CD longitudinal velocity (V_{CD}) and the shear velocity (V_{SH}) to calculate a value for the MD longitudinal velocity (V_{MD}).

$$V_{MD} = 2.82 (V_{SH})^2/V_{CD}. \quad (5)$$

The IPST robot for in-plane measurements has been used to measure the V_{MD}, V_{CD}, and V_{SH} along the CD of CD strips of several linerboard grades. The relationships of the measured velocity values were found to be consistent with a proportionality constant of approximately 2.8.

Analysis of Samples from April 1-4,1997 Pilot Machine Run at Herty

Thirty-four tests were run April 1-4, 1997 at the Herty Foundation in Savannah, GA. Rolls of paper to provide pulp for these tests were supplied by Georgia-Pacific from its Cedar Springs mill. An online measurement system (ABB 1190/SmartPlatform) is installed on the No. 1 pilot paper machine. However, measurements of paper properties used in this analysis were performed on the paper using instruments in the IPST laboratory under standard temperature and humidity conditions.

A table of the resulting values is included in this report. The values represent an average of all values taken of the given parameter for the given condition.

Statistical Analysis

Several statistical methods were used to analyze the data. Each paper property (i.e., ZD velocity, density, caliper, etc.) was tested to see whether the 6 available process changes had any effect on its value. The 6 process changes available at Herty are:

- Canadian Standard Freeness (CSF)
- 1st Wet Press
- 2nd Wet Press

- Wet Press Draws
- Calendering
- Basis Weight (BW)

The analysis begins by assuming that all variables (process changes) significantly affect the desired paper property. The statistical analysis will result in showing which effects probably occurred by chance and which effects probably occurred due to an actual relationship between process and property. The analysis uses an Excel macro and follows the procedures outlined above.

Seven paper properties (dependent variables) were examined and tested to determine which of the 6 process changes (independent variables) significantly affected them. The 7 paper properties examined were:

- Caliper
- Density
- Out-of-plane ultrasonic transit time
- ZD ultrasonic longitudinal velocity
- MD ultrasonic longitudinal velocity
- CD ultrasonic longitudinal velocity
- CD ultrasonic shear velocity

Results

Each independent variable was tested using the above described statistical analysis method. Outputs of the Excel macro for each test were obtained. The outputs for *Caliper* and *ZD ultrasonic transit time* are included in this report as examples together with a summary chart for all independent variables. The following is a brief discussion for each test.

Caliper:

The results show that caliper is highly influenced by basis weight. This is expected. If one assumes that all other process variables are held constant, an increase in basis weight should result in a thicker sheet. If calendering is used, the effects of basis weight will be reduced. Therefore, assuming everything is held constant, caliper should behave fairly linearly with basis weight. The slope of the line being determined by the current calender pressure.

It makes sense then that calendering is also a significant variable in predicting caliper. Freeness appears to play a role also. Perhaps the more refined the pulp, the denser the fibers can pack. This would cause an increase in density (we therefore expect to see a relation between density and freeness) which would, at a given basis weight, accompany a reduction in caliper.

The wet presses have slight effects on the caliper. The 1st wet press is much less significant in affecting caliper than the 2nd wet press. It is interesting to point out that while the F-test concluded that the 1st wet press was a significant variable, the t-test found it to be insignificant.

This model's large F-ratio suggests that a large percentage of the information needed to predict caliper is found in the significant variables (CSF, 1st Wet Press, 2nd Wet Press, Calendering, and BW). The mean absolute error and the standard error of estimate are only 3% of the average caliper reading.

Density:

Most surprising of the density results is the fact that basis weight is not considered a significant variable in its prediction. The wet press draws are about as significant in

estimating density as they were for estimating caliper. The same reduction in significance in the 1st wet press relative to the 2nd wet press is observed.

Perhaps the basis weight effect for density is similar to that discussed for caliper. A given calendering results in a given densification of the sheet. Thus with calendering constant, changing basis weight only produces a thicker sheet at the same density. However changes in the calendering pressure directly increase/decrease the sheet density.

The freeness argument for significance is similar to that used for caliper. More refining of a pulp will allow a closer packing of fibers and hence a denser sheet.

The mean absolute error and standard error of estimate show that the estimate was within 4% of the average density of predicting the measured value. However, the lower F-ratio (as compared to caliper), as well as a low r^2 value, suggest that other process variables are needed to add missing information to the model to improve the estimates of density.

Out-of-plane ultrasonic transit time:

The out-of-plane ultrasonic transit time showed a highly significant influence of freeness (CSF), 1st wet press, 2nd wet press, and BW. CSF is by far the most significant process variable in predicting transit time that was analyzed in this study. This is consistent with the expected increased bonding between fibers at a lower freeness (higher refining).

An increase in calendering from 50 pli to 350 pli was found to be insignificant in its effect on transit time. However, the 1st and 2nd wet presses are highly significant in determining transit time. The BW role is not as clear and also not as significant a factor in predicting transit time.

This model results in a 5-6% average error of prediction. However, it has a very high F-ratio and high correlation constant. Perhaps the high error is due to the fact that the values used for CSF, the most significant variable, are only set points and not exact measurements. Continuous measurements of CSF were not readily available.

ZD ultrasonic longitudinal velocity:

The results for ZD ultrasonic longitudinal velocity are consistent with those obtained for caliper and transit time, since ZD velocity is the caliper divided by the transit time. As expected, ZD velocity is found to be most sensitive to CSF due to the effects discussed with transit time. The 1st and 2nd wet presses also affect ZD velocity similar to transit time. The relative significance of all three of these process parameters is less than that for transit time. Since their influences on caliper are so much less than transit time, the effective influence on caliper divided by the transit time is reduced.

It is interesting to note that BW is considered insignificant. BW was fairly significant for both caliper and transit time. Apparently the effects that BW has on each of these variables is similar. Therefore dividing one by the other effectively cancels out the effects of BW.

The model has only a 6% average error. Its F-ratio and r^2 values are very high but less than that of both transit time and caliper. Perhaps additional information is required to replace the canceled BW effects.

MD ultrasonic longitudinal velocity:

MD ultrasonic longitudinal velocity appears to be sensitive to the same parameters as ZD velocity. It is sensitive to CSF and insensitive to calendering. However, BW effects are much greater in predicting MD velocity than ZD velocity. It is noted that while the

2nd wet press is considered a significant variable for MD velocity, the 1st wet press is not.

This is the only property affected by wet press draws in this study. The ability to change the draw in this study was limited and the effect observed is quite small.

CD ultrasonic longitudinal velocity:

The only process variable in this study found to have a significant effect on CD velocity was Basis Weight. This model, with only BW, is not very accurate for predicting CD velocity. A very low F-ratio (although still in the significant range) and r^2 value suggest that several more process variables are needed to have enough information to predict CD velocity.

CD ultrasonic shear velocity:

CD ultrasonic shear velocity seems to have the same significant process variables as MD velocity. A high F-ratio and r^2 value tends to show that the information present in the process variables is sufficient to predict CD shear.

Status of On-machine Demonstration

The Institute has a Cooperative Agreement with the U.S. Department of Energy's Office of Industrial Technologies (DOE-OIT) for a project to develop and demonstrate commercially viable on-line ultrasonic velocity sensors. The project includes the implementation of two pilot-scale prototypes and a full-scale production system with the ability to measure both in-plane and out-of-plane (ZD) ultrasonic velocity.

IPST is prime contractor with cost-share participation by ABB Industrial Systems Inc., Columbus, Ohio, the Herty Foundation, Savannah, Georgia, and the Georgia-Pacific

Mill in Cedar Springs, Georgia. We are in the fourth year of a 5-year development and testing program.

An AccuRay® 1190™ System with a Smart Platform™ 1200 has been installed on the web handling system in the laboratory at IPST. A similar system is installed on a pilot machine at the Herty Foundation. A similar system is installed at the Georgia-Pacific Cedar Springs Mill. It has been operating on their paper machine #1 since April 1997. The sensor carriage in each of these scanners contains state-of-the-art basis weight, moisture, temperature, and caliper sensors. ABB has built and installed an in-plane sensor at IPST and at the Cedar Springs Mill; work continues on debugging and checkout. IPST has designed and built a ZD ultrasonic velocity sensor using transducers mounted in fluid-filled wheels. After an initial test at Herty, it was decided to redesign the wheel mounting modules so that the wheels could be steered during scanning. The redesigned modules are ready for testing.

REFERENCES

Aidun, C.K., "A Fundamental Opportunity to Improve Paper Forming," *Tappi J.* 79 (6): 55(1996).

Baum, G.A., Brennan, D.C., and Habeger, C.C., "Orthotropic Elastic Constants of Paper," *Tappi J.* 64 (8):97(1981).

Baum, G.A., Pers, K., Shepard, D.R., and Ave'Lallemant, T.R., "Wet Straining of Paper," *Tappi J.* 67 (5):100(1984).

Habeger, C.C., and Baum, G.A., "On-line Measurement of Paper Mechanical Properties," *Tappi J.* 69 (6): 106(1986).

Lantz, K.G., and Chase, L.M., "On-line Measurement and Control of Strength Properties," *Tappi J.* 71 (2): 75(1988).

APPENDIX

"Relationships between Elastic Constants" by C. Habeger

In the plane of the sheet, the general theory of orthotropic elasticity allows paper to have four independent elastic constants. To completely determine ultrasonic elastic responses, it therefore requires four different velocity measurements. To achieve full characterization in the laboratory, we routinely measure longitudinal velocities in the MD and in the CD along with shear velocities in the CD and at 45 degrees to the MD. On-line, it is impractical to make four independent velocity measurements. Thus, it appears that we are handicapped on-line. But, maybe there is a way out.

There is empirical evidence that paper, in practice, has only three independent elastic constants. That is, there seems to be a relationship between elastic constants that exists for paper but not for general orthotropic planar materials. This is called Campbell's relation. It is a rather elegant relationship that can be expressed in a number of relatively simple, equivalent forms. One is that the shear modulus is independent of angle to the MD. Armed with Campbell's relation, on-line characterization is simplified; properties not directly measured can be inferred.

A good deal of paper physics research remains in order to confirm or deny Campbell and to rationalize its existence or nonexistence. An ultrasonic technique development at IPST provides a better method for establishing all the in-plane elastic constants. This needs to be applied to a range of paper and other planar structures to firmly evaluate Campbell and its perhaps preferential role in paper. On the theoretical side, Schulgasser has shown that the Cox model (uniform strain and all stiffness from fiber elongation) along with a special fiber distribution function (wrapped Cauchy) gives Campbell. However, Cox is poor in the determination of Poisson and shear elastic properties, and its comment on Campbell (a relation between all elastic constants) is of little relevance. Later Schulgasser and Page demonstrated that a laminate model (uniform strain and sheet stiffness from all fiber stiffnesses) and a wrapped Cauchy distribution could reproduce all four of the experimental elastic constants with reasonable fiber properties. Since the data fitted complied with Campbell, this indicates that Campbell is consistent with the laminate model, wrapped Cauchy, and wood fibers.

However, the implications of the laminate model and various distributions for Campbell were not investigated explicitly. Thus, there is much work to be done. Does Campbell truly exist in paper to a better approximation than in other materials? If so, why and under what conditions?

Another remarkable characteristic of paper is that its in-plane, elastic properties maintain orthotropic symmetry even under circumstances in which orthotropy would be expected not to hold. Orthotropic symmetry can be broken in paper manufacture by misaligning fiber orientation and wet straining. However, experimentally, the sheet properties average so that the elastic constants have orthotropic symmetry about an intermediate axis. The same cannot be said for plastic sheets drawn in more than one direction.

The orthotropic and Campbell phenomena seem to demonstrate that paper is peculiar in that its elastic properties average in very simple ways. Why is this?

Summary

Condition	ABB Caliper (um)	ABB Caliper STD	ABB BW (g/m^2)	ABB BW STD	Normalized Transit Time (uS)	Density (g/m^3)	Normalized Transit Time STD	ZD Velocity (km/sec)	MD Long. Velocity (km/sec)	MD Long. Velocity STD
7A	304.1424	11.3910	157.2413	14.6234	0.9918923	516.9989217	0.0535385	0.3066	3.0437	0.0961
8	321.8218	11.7014	155.1191	13.3055	0.9757108	482.0030066	0.0540188	0.3298	3.0598	0.0675
9	342.8092	11.3476	143.0529	12.0011	0.9673088	417.2958891	0.0854386	0.3544	3.0990	0.0680
9A	398.5831	25.0921	223.9764	20.2840	0.9993077	561.9315259	0.0851846	0.3989	2.9743	0.0605
10	469.7381	11.1199	204.0260	19.3586	1.7389205	434.3398088	0.0966386	0.2701	2.8111	0.0842
10A	419.6929	20.5276	213.6784	19.1625	1.0849615	509.1303778	0.0467348	0.3868	3.0505	0.0725
11	412.5006	16.5292	206.4809	22.2927	1.7833745	500.5590192	0.1037447	0.2313	2.7753	0.0707
11A	398.9669	16.0577	206.7661	18.2257	0.9756778	518.2538389	0.0626396	0.4089	3.1267	0.0735
12	399.1375	13.7213	195.8577	19.4080	1.8025636	490.7024967	0.0918545	0.2214	2.8073	0.0652
12A	404.4207	15.0246	209.0344	18.9161	0.9899974	516.8736181	0.0683301	0.4085	3.1279	0.0676
13A	456.4695	27.6070	215.9162	20.7371	1.2571945	473.0134271	0.0472039	0.3631	2.9016	0.0547
14A	434.2324	18.6518	213.6922	21.1094	1.0401139	492.1148671	0.0495117	0.4175	3.0336	0.0789
15	405.9206	14.9499	206.6429	19.0094	0.8178511	509.0722191	0.0661883	0.4963	3.2252	0.0642
16	357.3211	14.0547	209.6983	19.0497	0.8071866	586.8624453	0.0566696	0.4427	3.1836	0.0693
17	356.8030	15.5087	212.2328	19.3736	0.7452043	594.8176959	0.0540619	0.4788	3.1290	0.0638
18	393.8632	16.9037	208.3843	19.1898	0.7423495	529.0777817	0.0639828	0.5306	3.1776	0.0892
19	321.8349	9.7823	158.4639	11.4798	0.9033099	492.3764035	0.0564551	0.3563	3.2642	0.0647
20	300.7421	8.5084	164.3881	12.9281	0.8038022	546.6082002	0.0404130	0.3741	3.2630	0.0639
21	293.1167	8.2923	158.5692	12.2901	0.8037007	540.9763070	0.0406471	0.3647	3.3297	0.0635
22	327.7736	10.3754	156.3106	11.3234	0.7659669	476.8858517	0.0585669	0.4279	3.4009	0.0656
23	302.9714	12.4713	155.1911	11.0679	0.5219740	512.2302789	0.0557982	0.5804	3.5580	0.0707
24	290.9230	11.2525	156.3285	11.2901	0.5199370	537.3533992	0.0517407	0.5595	3.5106	0.0565
25	254.3619	8.9826	156.0490	11.2756	0.5487643	613.4918041	0.0360853	0.4635	3.3827	0.0675
26	253.2102	9.3934	154.9475	11.2157	0.5129519	611.9321642	0.0357597	0.4936	3.3551	0.0615
27	277.7952	10.3405	152.2453	10.8646	0.4925182	548.0487655	0.0499818	0.5640	3.3890	0.0615
28	405.1571	13.6912	198.6855	14.4638	1.0044901	490.3913199	0.0684950	0.4033	3.2668	0.0745
29	366.7159	12.4737	199.3126	14.0581	1.0219057	543.5068632	0.0524151	0.3589	3.2107	0.0549
30	383.0372	12.6415	198.8704	14.1446	1.0758974	519.1933876	0.0540806	0.3560	3.3023	0.0856
31	405.7879	13.2952	196.2461	13.8952	1.0529477	483.6173771	0.0701083	0.3854	3.3402	0.0631
32	366.1179	16.3461	191.9357	13.3690	0.7243349	524.2455159	0.0681675	0.5055	3.4950	0.0537
33	420.4867	16.5777	227.0863	17.0368	0.7683766	540.0559662	0.0429898	0.5472	3.2635	0.0712
34	397.1787	20.6917	226.6390	17.5173	0.7493601	570.6223538	0.0542564	0.5300	3.2778	0.0748
35	372.7285	26.7884	199.1671	15.4102	0.6209324	534.3490783	0.0425507	0.6003	3.3552	0.0803
36	360.2876	14.7821	198.0373	14.6500	0.6193663	549.6644539	0.0530000	0.5817	3.3693	0.0673

Summary

Condition	CD Long. Velocity (km/sec)	CD Long. Velocity STD	CD Shear Velocity (km/sec)	CD Shear Velocity STD	CSF (mL)	1st Wet Press (pli)	2nd Wet Press (pli)	Wet Press Draws (%)	Calendering (pli)	BW (g/m^2)
7A	2.0105	0.0383	1.4850	0.0161	650	490	980	1.2	350	157.2413
8	2.0352	0.0384	1.4916	0.0168	650	490	980	0.6	350	155.1191
9	2.0448	0.0308	1.4941	0.0138	650	490	980	0.6	50	143.0529
9A	2.1893	0.0529	1.5585	0.0260	497	490	300	0.6	350	223.9764
10	1.9608	0.0413	1.4009	0.0152	650	150	300	0.6	50	204.0260
10A	2.1846	0.0513	1.5575	0.0211	497	490	300	0.6	50	213.6784
11	1.9059	0.0417	1.3938	0.0184	650	150	300	0.6	350	206.4809
11A	2.1879	0.0501	1.5808	0.0204	497	150	980	0.6	50	206.7661
12	1.8852	0.0410	1.3818	0.0187	650	150	300	1.2	350	195.8577
12A	2.1540	0.0432	1.5688	0.0196	497	150	980	1.2	50	209.0344
13A	2.0529	0.0503	1.4764	0.0167	497	150	300	1.2	50	215.9162
14A	2.0909	0.0529	1.5171	0.0172	497	490	300	1.2	50	213.6922
15	2.2212	0.0456	1.6110	0.0148	497	490	980	1.2	50	206.6429
16	2.2229	0.0501	1.6164	0.0214	497	490	980	1.2	350	209.6983
17	2.2136	0.0531	1.6047	0.0203	497	490	980	0.6	350	212.2328
18	2.2651	0.0383	1.6251	0.0181	497	490	980	0.6	50	208.3843
19	2.2197	0.0335	1.6057	0.0151	450	150	300	0.6	50	158.4639
20	2.1752	0.0315	1.5999	0.0155	450	150	300	0.6	350	164.3881
21	2.1625	0.0345	1.5996	0.0119	450	150	300	1.2	350	158.5692
22	2.2141	0.0403	1.6232	0.0134	450	150	300	1.2	50	156.3106
23	2.3033	0.0339	1.6981	0.0162	450	490	980	1.2	50	155.1911
24	2.2511	0.0408	1.6743	0.0179	450	490	980	1.2	50	156.3285
25	2.2076	0.0355	1.6441	0.0193	450	490	980	1.2	350	156.0490
26	2.2340	0.0328	1.6579	0.0182	450	490	980	0.6	350	154.9475
27	2.2526	0.0345	1.6573	0.0171	450	490	980	0.6	50	152.2453
28	2.2648	0.0493	1.6293	0.0223	450	150	300	0.6	50	198.6855
29	2.2398	0.0335	1.6169	0.0163	450	150	300	0.6	350	199.3126
30	2.2128	0.0398	1.6084	0.0190	450	150	300	1.2	350	198.8704
31	2.2121	0.0391	1.6174	0.0195	450	150	300	1.2	50	196.2461
32	2.3359	0.0365	1.6996	0.0207	450	490	980	1.2	50	191.9357
33	2.2284	0.0376	1.6305	0.0219	450	490	980	1.2	50	227.0863
34	2.2410	0.0424	1.6332	0.0242	450	490	980	1.2	350	226.6390
35	2.2868	0.0391	1.6724	0.0167	450	490	980	0.6	350	199.1671
36	2.2860	0.0399	1.6693	0.0199	450	490	980	0.6	50	198.0373

Caliper Sensitivity Analysis

Multiple Regression Analysis
Dependant Variable: ABB Caliper (um)

Parameter	Estimate	Standard Error	T Statistic	P-Value
CONSTANT	-39.5314644	24.3293009	1.625	0.1150
CSF (mL)	0.2468233	0.0310597	7.947	0.0000
2nd Wet Press (pli)	-0.0383046	0.0066803	5.734	0.0000
Calendering (pli)	-0.1261851	0.0151613	8.323	0.0000
BW (g/m^2)	1.7417732	0.0865238	20.131	0.0000

Analysis of Variance

Source	Sum of Squares	DF	Mean Square	F-Ratio	P-Value
Model	100189.4174683	4	25047.3543671	149.00	0.0000
Residual	4875.0998615	29	168.1068918		
Total (Corr.)	105064.5173298	33			

R-squared (%)=	95.3599
R-squared [adjusted for d.f.] (%) =	94.7199
Standard Error of Est. =	12.9656042
Mean absolute error =	9.6240114

Further ANOVA for Variables (Assuming Each is last to be Added to Model)

Source	Sum of Squares	DF	Mean Square	F-Ratio	P-Value
CSF (mL)	10616.0278726	1	10616.0278726	63.15	0.0000
2nd Wet Press (pli)	5527.1539899	1	5527.1539899	32.88	0.0000
Calendering (pli)	11644.6382972	1	11644.6382972	69.27	0.0000
BW (g/m^2)	68123.6168859	1	68123.6168859	405.24	0.0000

Insignificant Variables at 0.95 criteria	P Value (F-Test)	P Value (T-Test)
Wet Press Draws (%)	0.4705	0.4705
1st Wet Press (pli)	0.1241	0.1241

Transit Time Sensitivity Analysis

Multiple Regression Analysis
Dependant Variable: Normalized Transit Time (uS)

Parameter	Estimate	Standard Error	T Statistic	P-Value
CONSTANT	-0.9985186	0.1341419	7.444	0.0000
CSF (mL)	0.0030946	0.0001691	18.305	0.0000
1st Wet Press (pli)	-0.0005884	0.0001031	5.706	0.0000
2nd Wet Press (pli)	-0.0003080	0.0000517	5.960	0.0000
BW (g/m^2)	0.0041657	0.0004785	8.706	0.0000

Analysis of Variance

Source	Sum of Squares	DF	Mean Square	F-Ratio	P-Value
Model	3.4974965	4	0.8743741	171.01	0.0000
Residual	0.1482782	29	0.0051130		
Total (Corr.)	3.6457746	33			

R-squared (%)=	95.9329
R-squared [adjusted for d.f.] (%) =	95.3719
Standard Error of Est. =	0.0715055
Mean absolute error =	0.0541953

Further ANOVA for Variables (Assuming Each is last to be Added to Model)

Source	Sum of Squares	DF	Mean Square	F-Ratio	P-Value
CSF (mL)	1.7133125	1	1.7133125	335.09	0.0000
1st Wet Press (pli)	0.1664533	1	0.1664533	32.55	0.0000
2nd Wet Press (pli)	0.1816093	1	0.1816093	35.52	0.0000
BW (g/m^2)	0.3875804	1	0.3875804	75.80	0.0000

Insignificant Variables at 0.95 criteria	P Value (F-Test)	P Value (T-Test)
Calendering (pli)	0.5285	0.5285
Wet Press Draws (%)	0.1772	0.1772

Summary of Sensitivity Analysis

Paper Property	Significant Process Parameters	F-Ratio	P-Value
Caliper	CSF	63.15	0.0000
	2nd Wet Press	32.88	0.0000
	Calendaring	69.27	0.0000
	BW	405.24	0.0000
Density	CSF	49.68	0.0000
	2nd Wet Press	21.11	0.0001
	Calendaring	53.67	0.0000
Out-of-plane ultrasonic transit time	CSF	335.09	0.0000
	1st Wet Press	32.55	0.0000
	2nd Wet Press	35.52	0.0000
	BW	75.80	0.0000
ZD ultrasonic longitudinal velocity	CSF	124.98	0.0000
	1st Wet Press	19.70	0.0001
	2nd Wet Press	23.67	0.0000
	Calendaring	7.61	0.0099
MD ultrasonic longitudinal velocity	CSF	163.18	0.0000
	2nd Wet Press	22.57	0.0000
	BW	45.50	0.0000
CD ultrasonic longitudinal velocity	CSF	226.82	0.0000
	2nd Wet Press	30.68	0.0000
	Wet Press Draws	6.17	0.0188
CD ultrasonic shear velocity	CSF	329.97	0.0000
	2nd Wet Press	57.37	0.0000
	BW	9.04	0.0053

FUNDAMENTALS OF ACOUSTIC RADIATION PRESSURE

STATUS REPORT

FOR

PROJECT F008

Pierre Brodeur
Joseph Gerhardstein
Feler Bose
Brian Pufahl

Institute of Paper Science and Technology
500 10th Street, N. W.
Atlanta, Georgia 30318

DUES-FUNDED PROJECT SUMMARY

Project Title: FUNDAMENTALS OF ACOUSTIC RADIATION PRESSURE
Project Code: FARPE
Project Number: F008
PAC: Paper Physics
Division: Fiber and Paper Physics Division
Project Staff
Faculty/Senior Staff: Pierre Brodeur
Staff: Joseph Gerhardstein (Assistant Engineer)
Feler Bose (Assistant Engineer)
Brian Pufahl (Assistant Engineer)
Mee Choi (Postdoc)
FY 97-98 Budget: $97,077
Allocated as Matching Funds: $97,077
Time Allocation
Faculty/Senior Staff: Pierre Brodeur (12%)
Support: Joseph Gerhardstein (19%), Feler Bose (24%), Mee Choi (10%), Brian Pufahl (7%)
Supporting Research
M.S. Students: None
Ph.D. Students: None
Related External Funding:

- Project #4183 "Acoustic Separation Technology" - Sponsored by Department of Energy and Beloit Corporation
- Project #4190 "Closed Water Treatment in Pulp Mills Using A Dual Flocculation/Ultrasonic Clarification Method" - Sponsored by State of Georgia Traditional Industry Program in Pulp and Paper - In collaboration with Prof. Yulin Deng (IPST Engineering and Papermaking Division)

RESEARCH LINES/ROADMAPS: 4, 7, 11, 12, and 13

PROJECT OBJECTIVES:

- Investigate fundamentals of acoustic radiation pressure (ARP) effects on fiber suspensions
- Demonstrate selected pulp and paper industry-related applications of acoustic radiation pressure
- Determine economic viability of acoustically-based processes

PROJECT BACKGROUND:

Project F008 was initiated in July 1992 to explore various effects of acoustic radiation pressure on water-suspended wood pulp fibers and other particulate matter. Since then, considerable work was accomplished to develop a structured research program, develop specialized test equipment (e.g., 450 l/min acoustic separation system) , perform preliminary demonstrations (e.g., transverse deflection of fiber suspensions subjected to traveling and standing ultrasonic wave fields in laminar and turbulent flows , acousto-optical method to determine wet compactibility of fiber suspensions), and seek external funding to supplement IPST's funding effort. Combined funding from all sources enables the following nonproprietary current activities:

- Acoustic separation of vessel elements and hardwood fibers (#F008)
- Development of automated image analysis method to quantify the presence of vessel elements in hardwood furnishes (#F008)
- Demonstration of dual chemical flocculation/ultrasonic clarification method (#4190)
- Theoretical/numerical analysis of acoustic radiation force acting on wood pulp fibers under zero flow, laminar flow, and turbulent flow conditions (#4183)
- Separation technology development (#4183)
- Safety analysis (#4183)
- Economical, technical, and energy assessments of technology (#4183);
- Technology transfer (#4183)

As indicated above, project F008 focuses on the vessel elements/hardwood fibers separation application.

SUMMARY OF RESULTS (March 97 - March 98):

- Preliminary vessel separation experiments were performed in April-May using Eucalyptus furnish and a newly-developed 450 l/min experimental setup (student work performed by Michelle Oakland, M.S., June 97); results provided evidence that the acoustic force produced in a traveling ultrasonic wave field propagating in a direction normal to a pulp stream can be used to get a vessel-depleted pulp stream and a vessel-enriched pulp stream; however, the lack of a rapid test method for vessel counting significantly affected the pace of work and prevented any optimization work.

- Another series of experiments was performed in November using oak furnish and test conditions similar to the first set of experiments; results were marginal and further demonstrated that the lack of a rapid and operator-independent vessel counting method was essential to the satisfactory demonstration of the separation method.
- Microscopy/staining work to enhance vessel/fiber contrast and preliminary software detection trials were initiated in November as preliminary steps toward the development of an automated vessel detection method using a high resolution CCD camera received in January. The method will provide the total number of vessels and vessel size distribution. It is a prerequisite to the satisfactory continuation of separation work.
- The separation system was upgraded in the December-March period in preparation for the next round of experiments. Also, test equipment is now available to determine power consumption.
- A study of ultrasonic refining of pulp suspensions was completed by John Blanz (M.S., June 97). Results were compared to measurements obtained using a PFI mill. In addition to refining results, it was found that ultrasonic cavitation is very efficient in removing fiber curl.

PROJECT GOALS FOR FY 98-99:

- Complete development of automated image analysis system to determine the percentage of vessel elements in hardwood furnish
- Complete demonstration of acoustic separation of vessel elements and hardwood fibers
- Provide assessment of separation application

PROJECT DELIVERABLES:

- Demonstration of acoustic separation of vessel elements and hardwood fibers
- Automated image analysis system for vessel counting and vessel size distribution

PROJECT SCHEDULE:

Tasks	FY 97-98						FY 98-99					
	Jul Aug	Sep Oct	Nov Dec	Jan Feb	Mar Apr	May Jun	Jul Aug	Sep Oct	Nov Dec	Jan Feb	Mar Apr	May Jun
Equipment Purchasing		---	---				---					
System Upgrading				---	---		---	---		---		
Microscopy/Staining Work			---	---	---							
Vessel Detection Method				---	---	---	---					
Prelim. Trials (Training)		---	---									
Vessel Separation Experim.				---	---	---	---	---	---	---	---	
Application Assessment										---	---	
Final Report											---	---

1. Introduction

This status report presents an overview of the progress accomplished so far in project F008. First, background information from the early days of the project is provided in Section 2 to appreciate current research activities. Section 3 provides a description of the experimental setup used to demonstrate the separation of vessel elements and hardwood fibers. Section 4 provides an introduction to the theoretical/modeling research effort on fibers interacting with an ultrasonic wave field. Section 5 provides a review of accomplishments about the separation of vessels and hardwood fibers. Finally, Section 6 summarizes research activities concerning the development of the automated image analysis method for vessel detection.

2. Background

Project F008 began in July 1992. This project was set up to study the fundamentals of acoustic radiation pressure effects on fiber suspensions and investigate potential applications in the pulp and paper industry. In essence, when water-suspended wood pulp fibers interact with an ultrasonic wave field, they are subjected to an acoustic force which results in fiber migration [1-4]. There is also an acoustic torque which reorients fibers. Both acoustic force and torque are nonlinear effects. These effects are very attractive because they enable the non-contact mechanical manipulation of flowing fibers. Although several studies have shown that fluid-suspended particles can agglomerate when submitted to traveling or stationary ultrasonic wave fields, very little is known in the context of prolate spheroids (cigar-shaped particles) or cylindrical

particles. Also, the study of fiber suspensions interacting with an ultrasonic wave field in laminar and turbulent flows is not documented in the literature. An understanding of acoustic manipulation of fibers at large flow rates is of primary importance.

Very early in the project, a basic experimental apparatus was built to investigate the acoustic force on non-moving and flowing fiber suspensions. A special acoustic cell mounted in an unpressurized vertical pipe of square crosssection was devised to deflect an input stream of fibers interacting with a traveling ultrasonic wave field (unidirectional field) normal to the flow direction. The cell is composed of a 2 x 10 cm active area piezoelectric ceramic transducer operating at 150 kHz and a sound absorber of equivalent area. In this arrangement, fibers flow against gravity and deflect toward the absorber position when the sound field is turned on. The transducer-absorber separation distance is 2 cm.

Preliminary experimental observations confirmed that the acoustic force could potentially be used to separate/fractionate fibers based on fiber width [5]. Consequently, an in-flow divider blade was installed above the acoustic cell in such a way as to separate highly deflected fibers (coarse fibers) from weakly deflected or undeflected fibers (slender fibers and/or fines). This would lead to at least two output streams: a coarse fiber-enriched stream and a coarse fiber-depleted stream. Literature/patent searches did not reveal evidence of past work in this area. A patent application was filed by IPST in 1996.

In a particular series of experiments using the basic experimental setup, rayon fibers of constant width/variable length and constant length/variable width were tested as a

function of acoustic intensity and flow rate at 0.05% consistency. Rayon fibers were used as they best simulate wood pulp fibers. Separation efficiency was indirectly determined by measuring the cleanliness efficiency of the weakly deflected fiber output stream, i.e., by analyzing the percentage of fibers remaining in the "clean stream." Cleanliness efficiency [CE] is defined as follows:

$$CE = 100(1 - f_C/f_F) \quad [1]$$

where f_C and f_F refer to the percentage by weight of solids oven dried for the clean and feed streams, respectively.

Results supporting the hypothesis that fiber migration is a function of fiber width are shown in Figures 1 and 2. While the cleanliness efficiency increases as a function of intensity for all test samples (at constant flow rate), indicating an increased migration rate from the transducer to the absorber, the cleanliness efficiency is not significantly affected by fiber length in Figure 1 and increases as a function of fiber width in Figure 2.

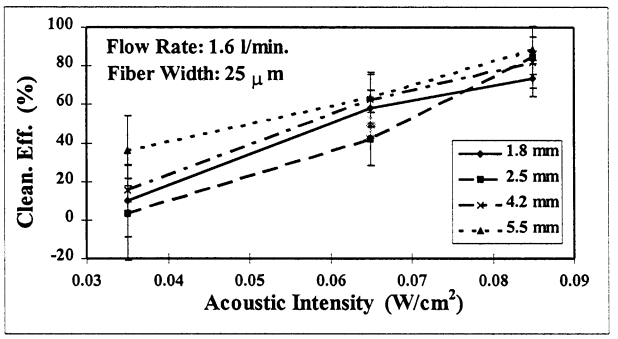

Figure 1. Cleanliness efficiency as a function of acoustic intensity for constant width/variable length rayon fibers. Fiber dimensions were determined a priori using a microscopy method.

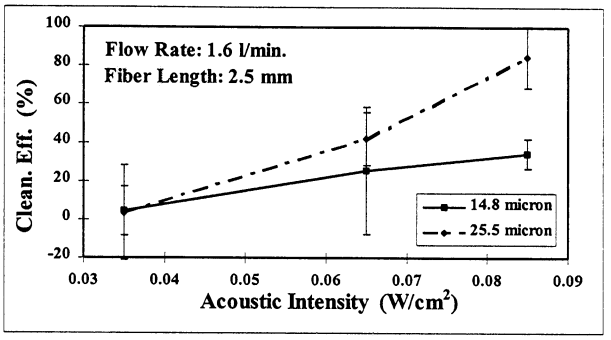

Figure 2. Cleanliness efficiency as a function of acoustic intensity for constant length/variable width rayon fibers.

In a similar set of experiments, a Bauer-McNett classifier was used to separate two fractions of never-dried hardwood fibers (sample A, average fiber length: 0.78 mm; sample B, average fiber length: 1.10 mm). The cleanliness efficiency was determined for samples A and B and a mixture labeled M (25% A - 75% B; predicted fiber length: 1.02 mm). Results are presented in Figure 3. Clearly, the efficiency increases as a function of fiber length (related to fiber width in this case).

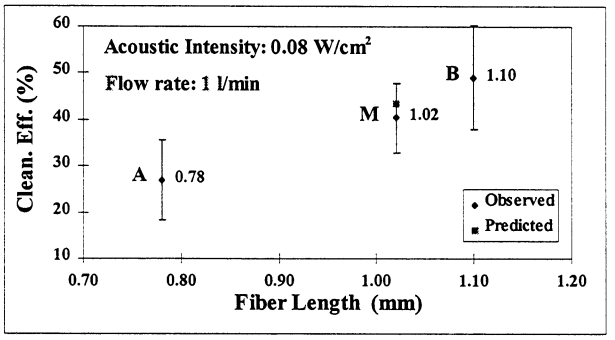

Figure 3. Cleanliness efficiency for samples of never-dried hardwood fibers.

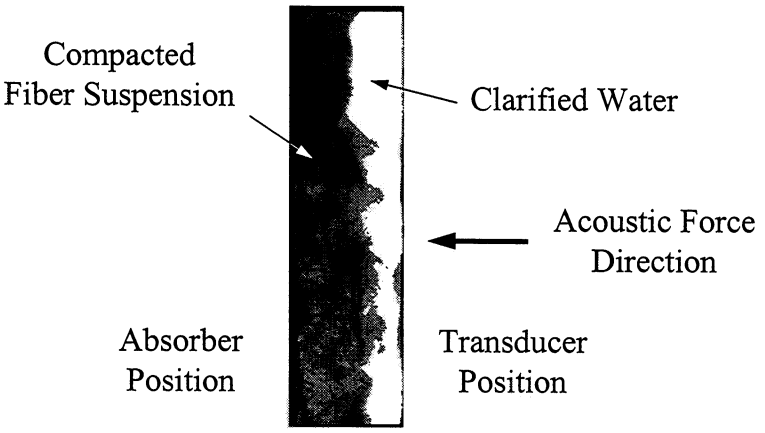

Figure 4. Pulp thickening effect [2 cm (horizontal) x 10 cm (vertical)].

Another series of observations was obtained using softwood fibers under zero-flow conditions to study the compactibility of fiber suspensions. Figure 4 shows a compacted fiber suspension for an initial pulp consistency of 1% (*white indicates water and black indicates fiber*). The acoustic intensity is 0.3 W/cm^2. One can easily see a pulp thickening effect. A new test method, acoustic wet fiber compactibility, has been proposed to control the refining process and predict the apparent density of paper [6].

Using a more efficient transducer (> 90% power efficiency conversion from electrical to mechanical power), video recordings were obtained for different acoustic intensity levels at 70 l/min (18 gal/min) using never-dried softwood fibers (at max. pump capacity; Re $\approx$ 6000 - turbulent regime). Results are shown in Figure 5 (*black indicates fiber*). Pulp consistency is 0.1%. One can see that fiber deflection (toward the left) significantly increases as a function of intensity (shown as a thickening of the fiber mat (*black*) on the left side of the cell). At 4 W/cm^2, the intensity is already too large and deflected fibers bounce back.

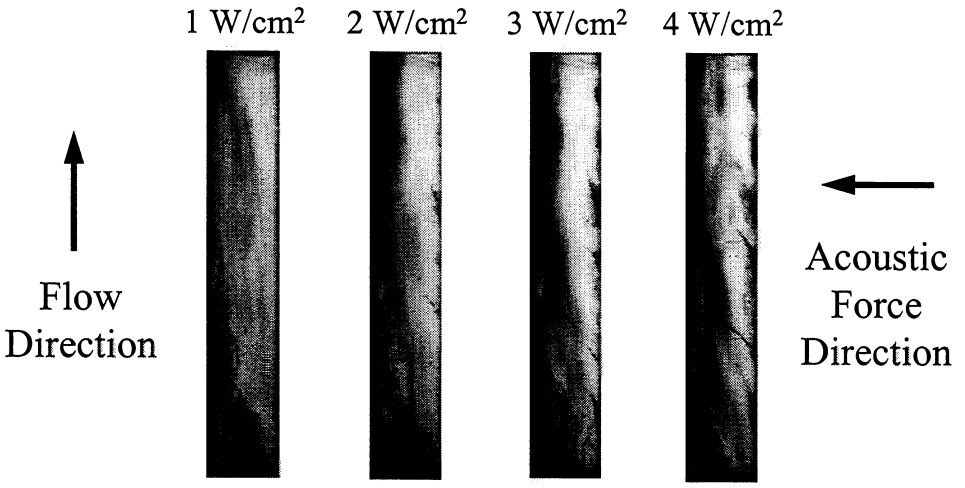

Figure 5. Video recordings under turbulent flow conditions. [2 cm (hor.) x 10 cm (vert.)].

Other test results can be summarized as follows:

(1) Migration rate for shives is significantly larger than that for fibers;

(2) Migration rate for earlywood fibers is larger than that for latewood fibers;

(3) Observations using OCC fibers show that the fiber fraction migrates but the fines do not; and

(4) Observations using mixtures of fibers and ink particles attached to air bubbles show that the air bubbles are not affected by the acoustic force, thus providing a means to enhance the removal of fibers in flotation deinking.

Experiments were also conducted using a standing ultrasonic wave field. This field is obtained by a reflector instead of an absorber. The reflector was made of stainless steel. Providing that the separation distance between the transducer and the reflector corresponds to n (l/2), where l is the acoustic wavelength (10 mm at ¦ = 150 kHz in

water), interference between the transmitted and reflected wavefronts produces a standing wave field pattern. Since the transducer-reflector separation distance was 2 cm, four nodal pressure planes were created. Observations using wood pulp fibers showed that the fibers quickly migrate toward pressure planes when the acoustic field is turned on, thus leading to the formation of four parallel agglomeration planes. This is illustrated in Figure 6.

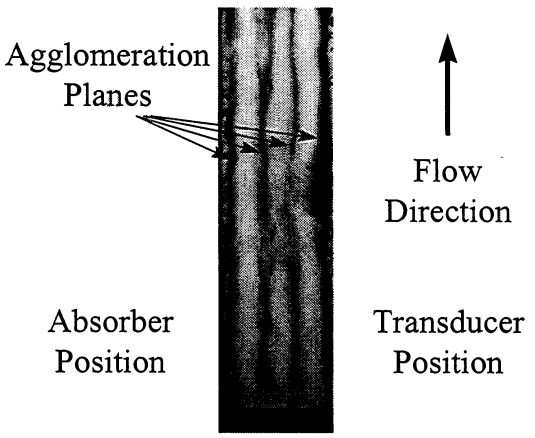

Figure 6. Agglomeration of 5.9 mm rayon fibers at 1% consistency in a standing wave field. Four layers are produced. The Reynold's number is approximately 500.

Technical limitations (small size of equipment, consistency and flow limitations) in the quest to perform realistic separation experiments using existing equipment led to the decision in 1996 to design and fabricate a larger-scale experimental setup. The separation system was functional in March 1997, but with limited capabilities. It was used to gather preliminary measurements on the separation of vessel elements and hardwood fibers [7]. Additional equipment to drive transducers and determine power

consumption was purchased during the fall of 1997. Details of this apparatus are reported in the next Section.

In parallel to the development of the larger-scale experimental setup and the vessel-fiber separation study, an investigation of ultrasonic refining of pulp suspensions using a 20-kHz ultrasonic processor was performed by John Blanz (M.S., June 1997) [8]. The most interesting finding was that high power ultrasonics can potentially be used to decurl fibers.

3. Ultrasonic Separation Apparatus (Joseph Gerhardstein)

Last year, a larger laboratory scale acoustic flow cell and flow loop was built to overcome problems with the smaller setup. Schematic diagrams of the flow loop and cell are shown in Figures 7 and 8, respectively.

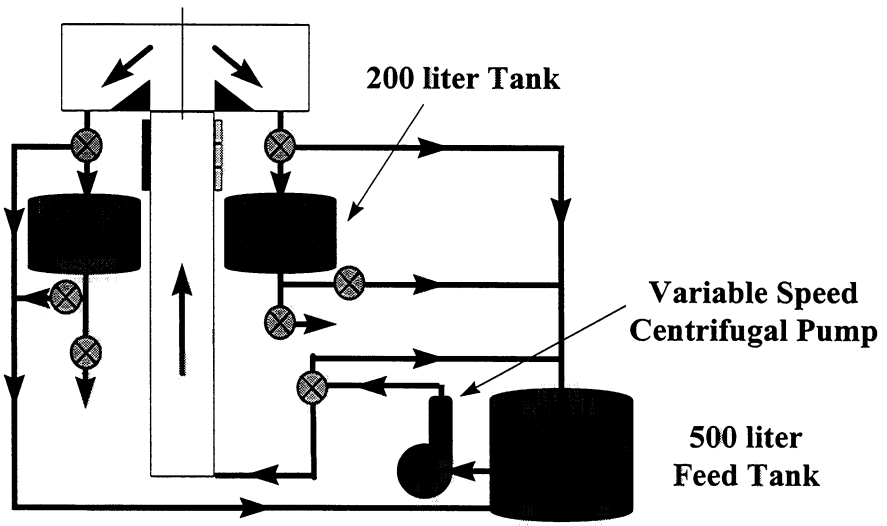

Figure 7. Flow system for the laboratory prototype acoustic separator (*drawing not to scale*).

Briefly, the flow cell consists of a 1.9-meter flow development section, an acoustic section containing three 5x10-cm, 150-kHz piezoelectric transducers above it, and is topped by an atmospheric pressure mechanical separation system. The flow cell is rectangular in cross section, with one dimension fixed at 5 cm, and the other variable from 5-15 cm (in 5 cm steps). A 450 l/min (maximum) variable speed centrifugal pump is used to produce flows in the cell with Reynolds numbers between 400 and 140,000. A 500 liter stock tank is used to feed the pump, and a pair of 200 liter stock tanks are on the output of the flow cell (one on each side). The cell is typically run in a close loop mode, where the stock flows from the 500 liter tank, through the pump, into the flow cell where it is acoustically processed, then out into one of the 200 liter tanks and back to the 500 liter tank (it can also be run in batch mode where the sample is entirely collected in the 200 liter tanks). Samples are usually taken from the 200 liter tanks while the cell is running in closed loop mode.

Figure 9 shows the electrical setup for the acoustic cell. Three separate channels are used, one for each transducer, to provide flexibility in how the system is run. A computer controls three function generators via a GPIB network. These function generators are set to produce sine waves at 150 kHz, and are phase locked so that the waves are synchronized. The output from the function generators are fed into three power amplifiers which boost the signal strength to the amplitude necessary to drive the transducers. As the output from the power amplifiers is at 50 ohms, and the transducers have a much larger input impedance, a set of matching networks is used to perform the transition. Feedback is provided to the computer from each power amplifier to maintain the power output constant during an experiment.

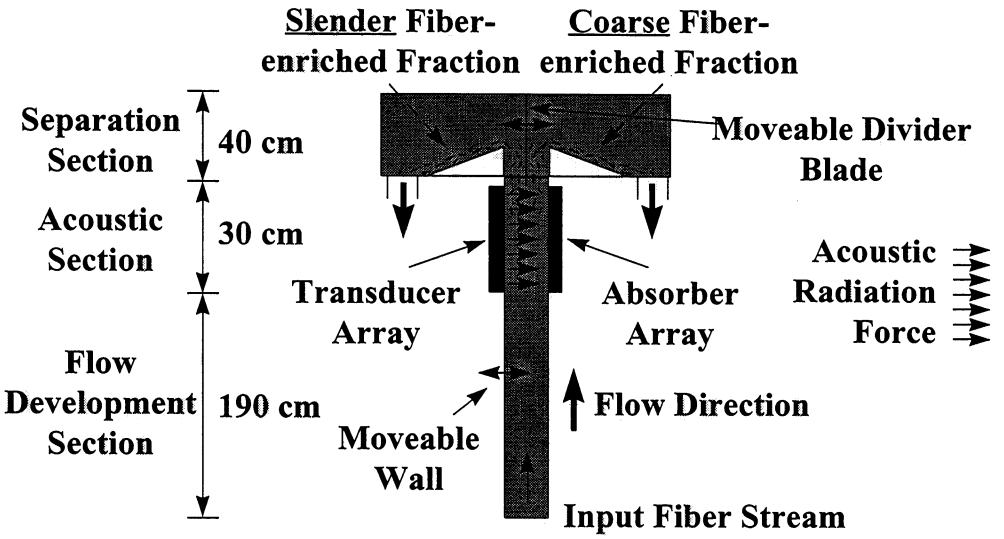

Figure 8. Schematic diagram of the laboratory prototype acoustic separation system (*drawing not to scale*). Separation using a traveling wave field (unidirectional) is shown.

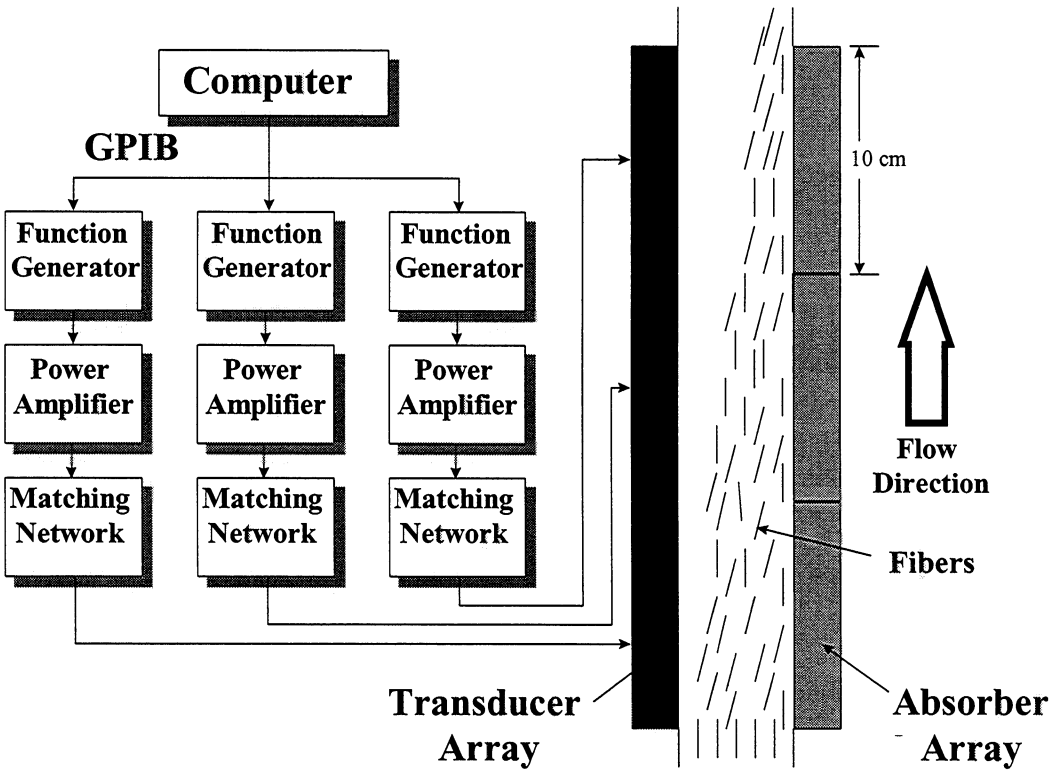

Figure 9. Electrical setup for the acoustic cell.

The laboratory scale acoustic separator has undergone extensive testing. Figure 10 shows an example of deflection of softwood kraft pulp using a traveling wave field configuration. However, experiments done last year by IPST M.S. student Michelle Oakland (M.S., June 1997) showed several limitations to the new system that needed to be corrected before further meaningful experiments could be done. Of primary concern was the power available from the current ENI power amplifiers. With the 400-watt amplifier used previously in the small scale setup, intensities of up to 20 watts/cm^2 could be generated in the small (2x10 cm) transducer (see previous section), but only 8 watts/cm^2 with the new, larger (5x10 cm) transducers. There was also only one 400-watt amplifier, and hence 100-watt amplifiers were used for the other two new transducers which produced intensities of only 2 watts/cm^2. These lower intensities made it difficult to repeat experiments done earlier on the smaller scale setup.

At the time this report was written, three new 1500-watt ENI power amplifiers had been ordered and were installed on the setup, which will now provide intensities of up to 30 watts/cm^2. Because of these higher intensities, the transducers and matching networks were returned to the manufacturer to have modifications made to increase their power handling. The transducers were designed to handle temperatures up to 100 °C, but because of the higher power that each transducer and matching network will be handling, overheating may become a problem (especially at low flow rates). To monitor temperature, a system of thermocouples has been installed on both the transducers and the matching networks, and a computer will be used to monitor the temperatures and shut down the system if overheating occurs.

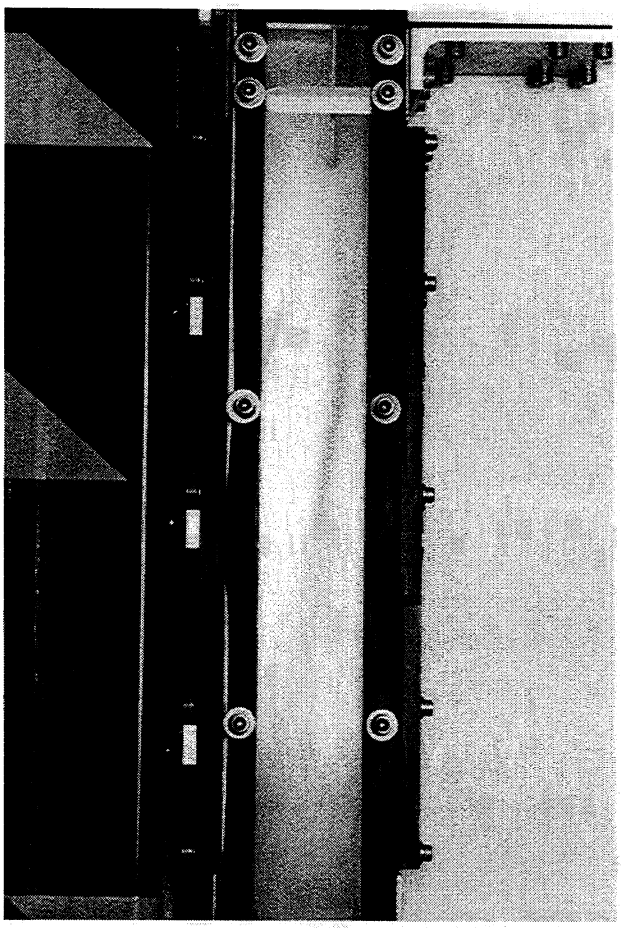

Figure 10. Softwood Kraft pulp in the new flow cell. Transducers are on the left, and absorbers on the right (traveling wave configuration); flow is from the bottom to the top. Note the mechanical separator at the top of the flow cell.

Heating in the transducers and matching networks is caused by inefficient power conversion. In order to determine where electrical power is being lost, an oscilloscope with high frequency current and voltage probes was purchased. This oscilloscope is used to measure current and voltage, and hence calculate power, along the electrical path from the wall outlet to the transducer as shown in Figure 11. Measurements will be done between the wall outlet and the power amplifier (amount of power the amplifier consumes), between the power amplifier and the matching network (amount of power

output by the amplifier), and between the matching network and the transducer (power delivered to the transducer).

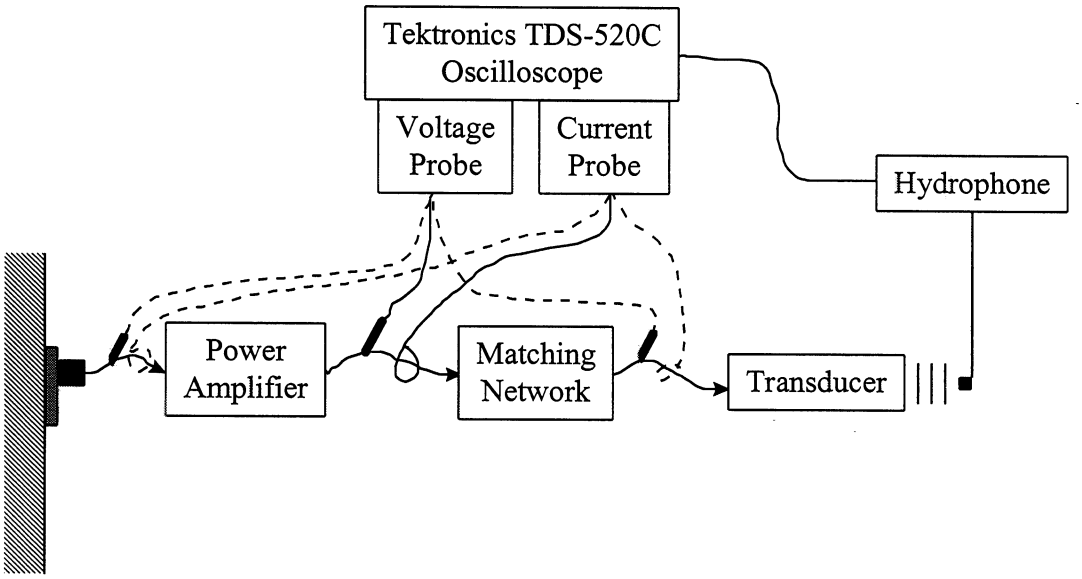

Figure 11. Measurement of electrical power usage from wall to transducer using new oscilloscope and high frequency probes. Oscilloscope is shown measuring power between Power Amplifier and Matching Network.

The power measurement setup has already been tested and yielded some unexpected results. Specifically, we were able to measure power between the Power Amplifier and Matching Network on the small scale setup. Upon looking at the waveform, it was noticed that the old ENI 400-watt power amplifier was not producing as clean of a sine wave as was hoped. Because frequencies other than 150 kHz are not efficiently used by the transducer, these other frequencies represent power that will be lost to heat in the transducer. After discussion with other users of this amplifier, it was determined that this is a characteristic of the amplifier. At the time this report was written, no measurements had been done with the new amplifiers (though other users of these

amplifiers were much happier with the signal quality). Measurements were attempted between the Matching Network and Transducer. However, because of the extremely high impedance of the transducer, large errors occurred in the measurements. We are currently working on a way to correct these errors or to increase the impedance of the oscilloscope probes.

In addition to measuring electrical power losses, a new hydrophone with an extra-long arm was ordered to measure the acoustic power within the flow cell and determine the electrical-to-acoustic power conversion efficiency of the transducers. This measurement will provide the final piece of information about power losses from the wall to the water, and should provide overall efficiency information.

Another avenue of increasing efficiency of the separation system is to use a standing wave field and take advantage of the resonance condition within the flow cell. However, with the current 150-kHz transducers, standing waves produce agglomeration planes separated by only 5 mm. This would make it difficult to perform mechanical separation after the pulp has left the flow cell. In order to increase the separation of the standing wave agglomeration planes, a set of 60-kHz transducers which will produce spacings of 12.5 mm was ordered recently. The frequency of 60-kHz was chosen as it will produce resonance in the flow cell with wall spacings of 5, 10, and 15 cm, and will have agglomeration planes spaced far enough apart to mechanically separate the pulp after the flow cell. The use of a standing wave field is attractive in the context of the separation of vessels and hardwood fibers (see Section 5) because vessels can be deflected over relatively shorter distances, thus enhancing separation efficiency.

4. Theoretical/Modeling Research Program (Mee Choi)

The experimental work is complemented by a newly-established theoretical/modeling research program. This program is especially important in order to optimize and/or predict various effects. It has the following initial objectives:

- Review past theoretical work about acoustic radiation pressure effects on cylindrical particles and prolate spheroids and verify that theoretical predictions agree with experimental observations.
- Develop a theoretical framework to begin the study of acoustic deflection of dilute fiber suspensions under different flow conditions

In agreement with the first objective, a review of different derivations for the acoustic force applied to rigid and elastic cylinders was undertaken. Derivations by Awatani [9] and Zhuk [10] (infinitely long rigid cylinder in traveling wave field with axis perpendicular to the sound field) and Hasegawa, et al. [11] (infinitely long elastic cylinder in traveling wave field with axis perpendicular to the sound field, including internal reflections and scattering) are compared in Figure 11.

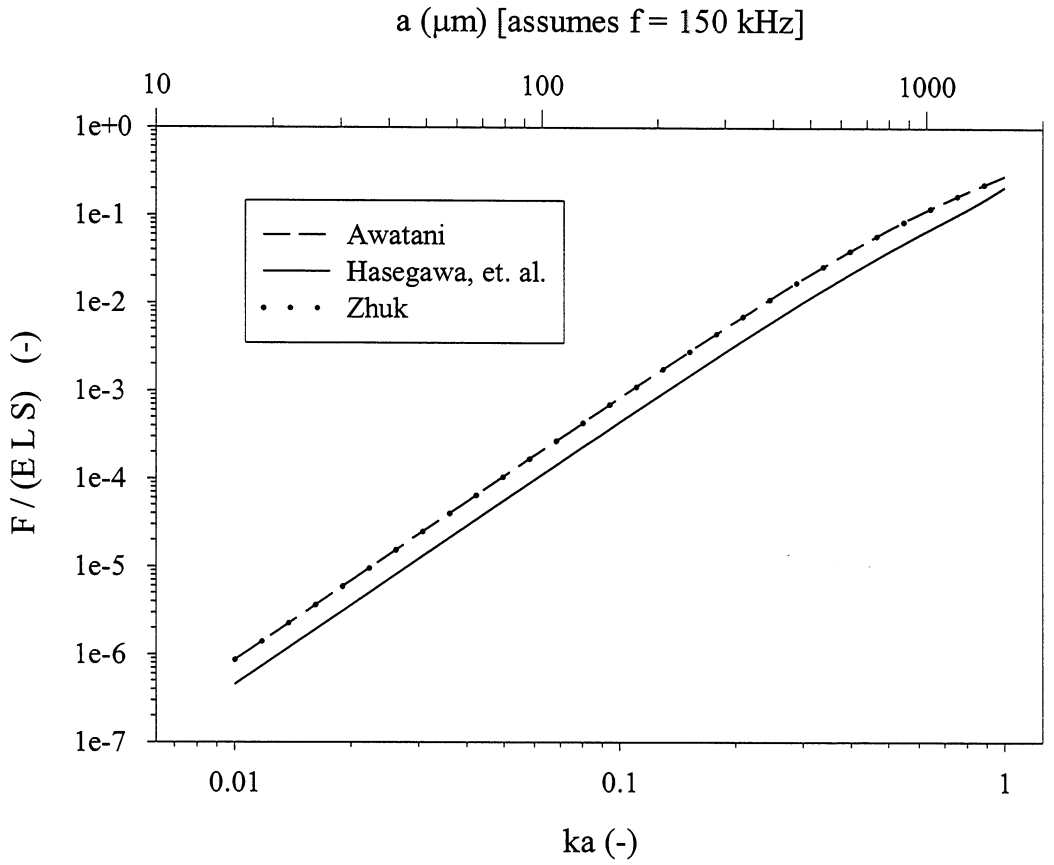

Figure 11. Plot of dimensionless acoustic radiation force vs. ka (also dimensionless) for the case of a traveling wave field as obtained using different equations. Upper axis is cylinder radius, a, in mm for a 150-kHz acoustic wave in water. Awatani [9] and Zhuk [10] give nearly identical results, hence overlap.

In this figure, the force (per unit length L, per unit surface area S, and per unit acoustic energy density E) is plotted as a function of the parameter ka where k is the wave number and a is the cylinder radius. Assuming water as the suspending medium and 150 kHz as the wave frequency, k = 628 m^{-1}. The density is set to 1090 kg/cm^3. It can be seen that in the range of ka of interest to us (ka = 0.01 to 0.1), the derivations agree very well with each other. From Figure 11, increasing ka will cause an increase in the

acoustic force. Increasing ka one order of magnitude (say from 0.01 to 0.1) will cause an increase in the acoustic force of approximately 2.5 orders of magnitude. This could also be interpreted as an increase of one order of magnitude in ka will reduce the amount of acoustic energy density (E), and therefore electrical power, by approximately 2.5 orders of magnitude. Hence it appears obvious that working in a ka range of 0.01 is not as efficient as working closer to a ka of 1. The value of ka can be increased one of two ways: an increase in the cylinder radius (a); or an increase in the acoustic wave frequency (increase in k). As the fiber dimensions are not easily changed, the most forward way to change ka is to increase the transducer frequency.

Figure 12 shows a comparison of the force for a traveling wave and a standing wave field, as derived by Awatani [9]. As can be seen, the force is significantly larger for the standing wave. Figure 13 plots the ratio between the standing wave force and the traveling wave force. For a "normal" fiber of 25 mm radius in water exposed to a 150-kHz sound field (ka = 0.0157), a standing wave will produce a force approximately 5000 times greater than the traveling wave. As ka approaches 1, the traveling wave and standing wave forces converge. Hence for low values of ka, the standing wave will produce a significantly stronger force than the traveling wave.

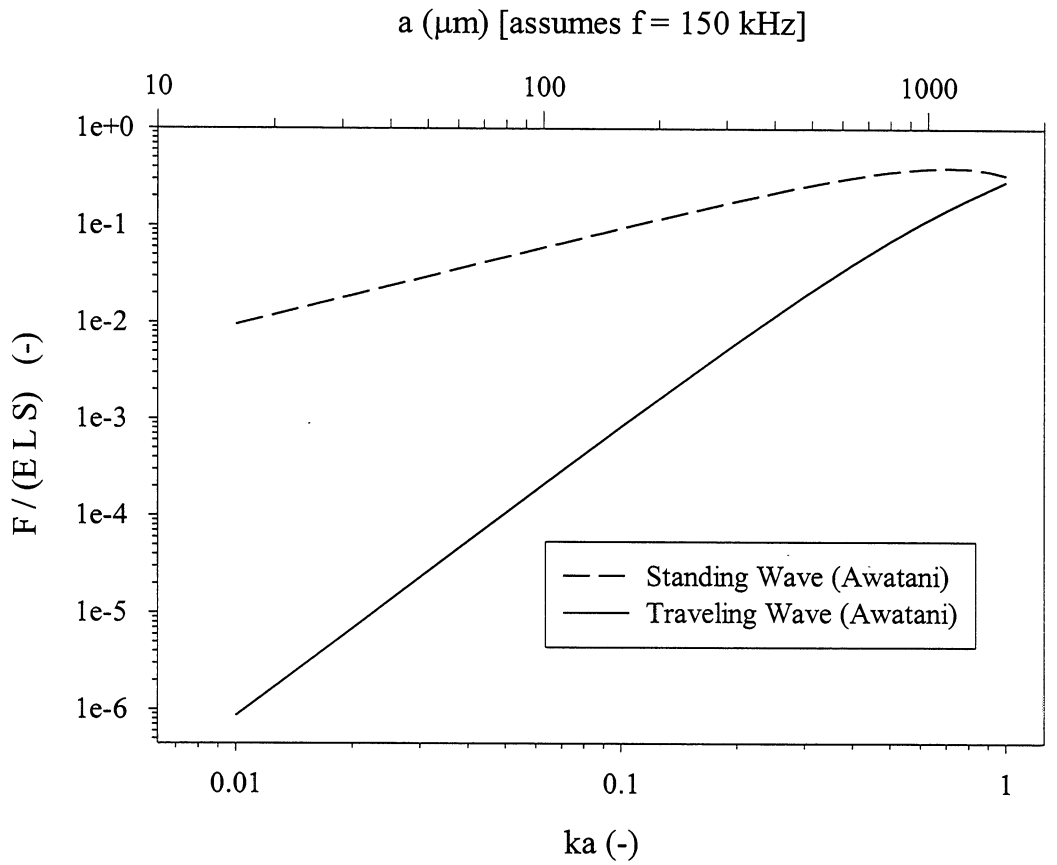

Figure 12. Comparison between acoustic radiation force for traveling and standing wave field, from Awatani [9]. It can be seen that the acoustic force for a traveling wave field is significantly larger.

Based upon the above theory, a series of experiments with extremely dilute solutions (0.0001%) is planned with the intent to measure the velocity of fibers in a suspension. In order to control the fiber properties (including length, diameter, and shape), rayon fibers will be used initially. A high-speed video system will be used to measure fiber translation and rotation speeds within standing and traveling wave fields for various values of ka in order to confirm the theoretical predictions.

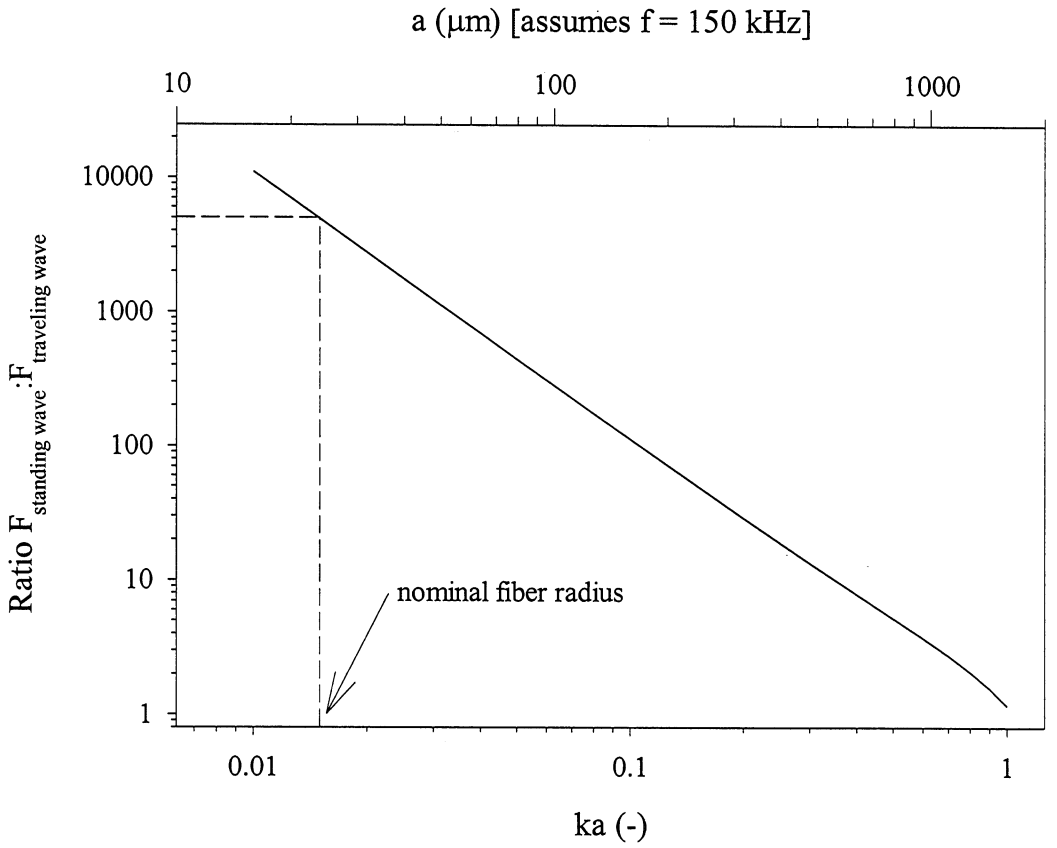

Figure 13. Ratio of Standing Wave acoustic force to Traveling Wave acoustic force, based on Awatani [9]. For a fiber with a 25 mm radius at 150 kHz, the ratio is approximately 5000:1.

5. Separation of Vessel Elements and Hardwood Fibers (Joseph Gerhardstein, Feler Bose)

At the Fall 1996 Project Advisory Committee meeting, it was recommended that an investigation of the use of acoustic radiation pressure principles to separate vessel elements and hardwood fibers be undertaken. It is well known that the presence of vessel elements during offset printing can be detrimental because vessels do not bond very well to fibers, and consequently, can be picked by impression cylinders (vessel picking problem). Since there are currently no satisfactory methods to remove vessel elements, the industry addresses the problem by using pulp mixtures to reduce the concentration of vessel elements. Also, refining is used to reduce the size of these particles but at the expense of unnecessary hardwood fiber treatment.

A preliminary study of acoustic separation of vessels and hardwood fibers was performed by Michelle Oakland (M.S., June 1997) during FY 1996-1997 [7]. Eucalyptus bleached kraft pulp (100%) from dry lap sheets was used for all experiments. As no current accepted method existed for counting vessels within a pulp, the first task was to develop a repeatable method to perform the quantification. The method was developed based upon industry-developed microscopy methods, as well as from the literature (no standard test method is available). The method involved placing 1.5 ml of well mixed 0.1% pulp slurry (for a total of 1.5 mg of pulp) onto a standard microscope slide. The slide was dried and then stained. Slides were placed under a 200x microscope, and the entire area under the coverslip was viewed in a systematic manner. Vessels were broken into four categories: Large Vessels (intact

vessels much larger than a fiber), Small Vessels (intact vessels about the size of a fiber), Large Pieces (vessel pieces larger than about 20x50 mm) and Small Pieces (vessel pieces smaller than about 20x50 mm). Slides were measured in a random order to reduce systematic error. Results were then reported as the number of vessels per 1.5 mg of pulp. Six slides were measured for each sample for statistics. A typical large eucalyptus vessel is shown in Figure 14.

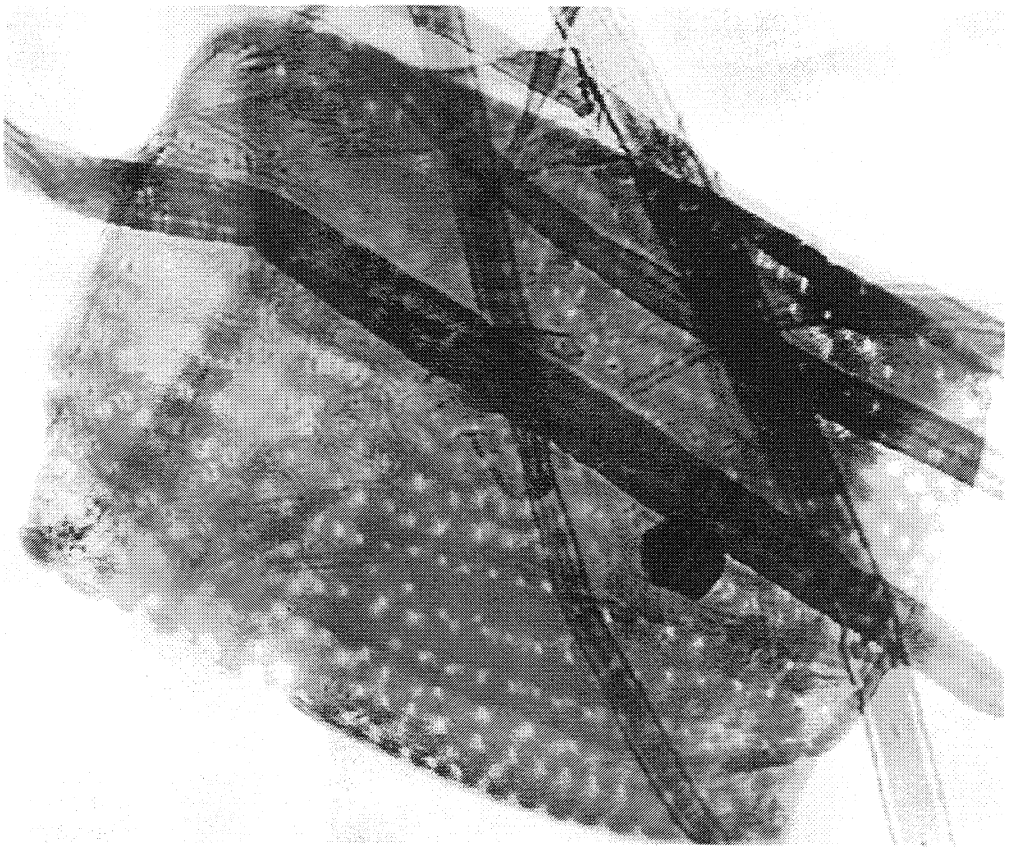

Figure 14. Typical large vessel found in eucalyptus pulp.

Four experiments were run using the eucalyptus pulp and the experimental setup previously described in Section 3 (note: the setup was not as complete as it is now). The experiments are detailed in Table I. Experiments A and B were repeats of each

other. Experiment C looked at reversing the acoustic intensity distribution from 9 W/cm^2 on the bottom transducer and 4 W/cm^2 on the top transducer to 4 W/cm^2 on the bottom and 9 W/cm^2 on the top transducer. Experiment D investigated lower consistency. All results are for the case of the mechanical divider placed 1 cm from the absorber side of the flow cell (4 cm from the transducer side).

Table I. Experimental Design for Vessel Separation Experiments.

Experiment Design	Consistency	Flow Rates (l/min)	Acoustic Intensity		
			Bottom Transducer (W/cm^2)	Middle Transducer (W/cm^2)	Top Transducer (W/cm^2)
A	0.20%	20, 50, 75, 100	9	4	4
B	0.20%	25, 100	9	4	4
C	0.20%	25, 100	4	4	9
D	0.10%	25, 100	9	4	4

Initially, more experiments were planned, especially at different flow rates, consistencies and acoustic intensities. However, the counting of vessels turned out to be quite time consuming, and seriously limited the number of experiments that could be done. Figure 15 shows results from Experiment A.

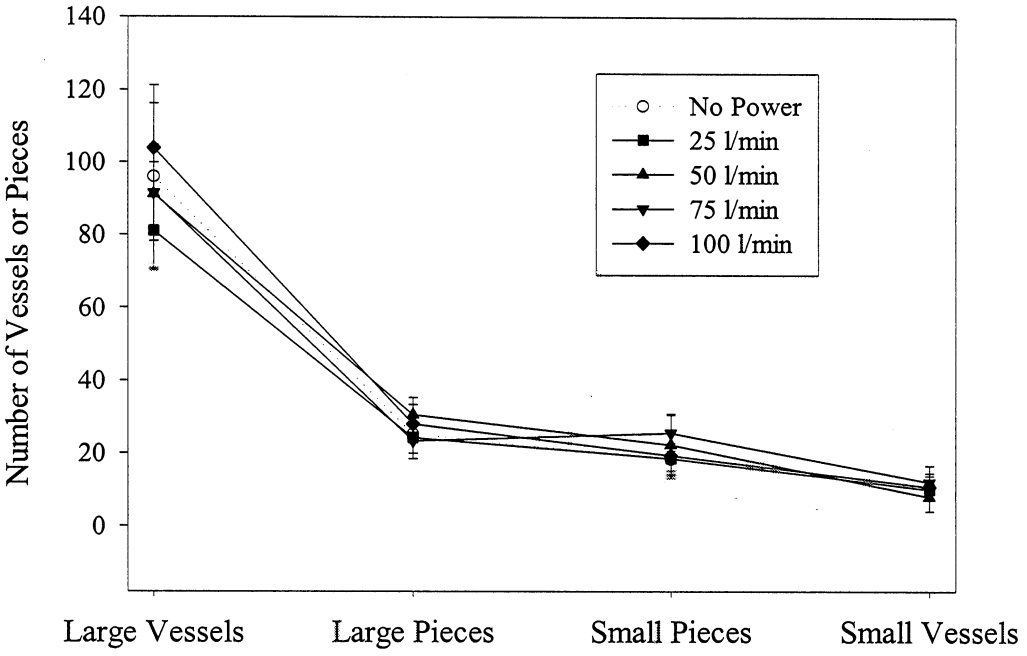

Figure 15. Results from Experiment A.

Only the large vessels appear to have any significant variation as a function of flow rate. For the large vessels, only the 100-L/min flow rate had a higher vessel count than the no power case, though the standard deviations easily overlap. Figure 16 shows results from all four experiments (note: for experiments B, C and D, data was taken only at 25 and 100 l/min). As the large vessels and large pieces were considered to be the most important (both from a vessel picking standpoint and an ARP standpoint), their counts were combined while the small vessels and small pieces counts were not used.

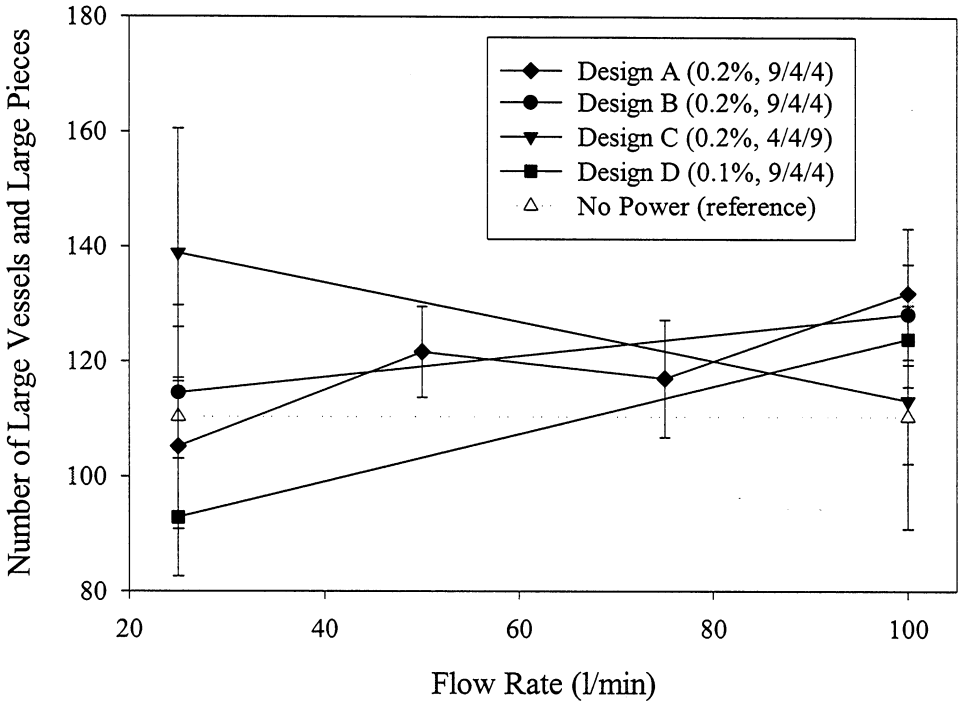

Figure 16. Flow Rate vs. Number of Large Vessels and Large Pieces for Experiments A-D. Dotted line is for samples taken with no acoustic field.

The results shown in Figure 16 are somewhat confusing. At the lowest flow rate where one would expect the best separation, the results are widely scattered around the no power case. However, at higher flow rates where one would expect worse separation, the results exceed the no power case and tend to converge. Also, experiment C has the opposite trend from experiments A, B, and D.

The results are explained as follows. For experiment C, fibers flowing through the acoustic cell see an increasing acoustic field (from 4 to 9 W/cm^2). The initial 4 W/cm^2

on the lower and middle transducers begins the migration of the vessels toward the absorber. The 9 W/cm^2 on the top transducer then pushes the vessels the rest of the way toward the absorber, resulting in a high vessel concentration at the mechanical divider. For experiments A, B and D, fibers flowing through the acoustic cell see a decreasing acoustic field (from 9 to 4 W/cm^2). Upon entering the cell, the vessels encounter the relatively strong 9 W/cm^2 field and are deflected toward the absorber. However, as they flow through the cell, the middle and top transducers do not apply as strong a field, and hence allow the vessels to spring back from the absorber and remix with the flow, resulting in a lower vessel concentration at the mechanical divider. This is shown in Figure 17. At a flow rate of 100 l/min, the results converge toward the no power case. This is believed to be due to insufficient dwell time within the acoustic cell to achieve separation because of the higher flow rate.

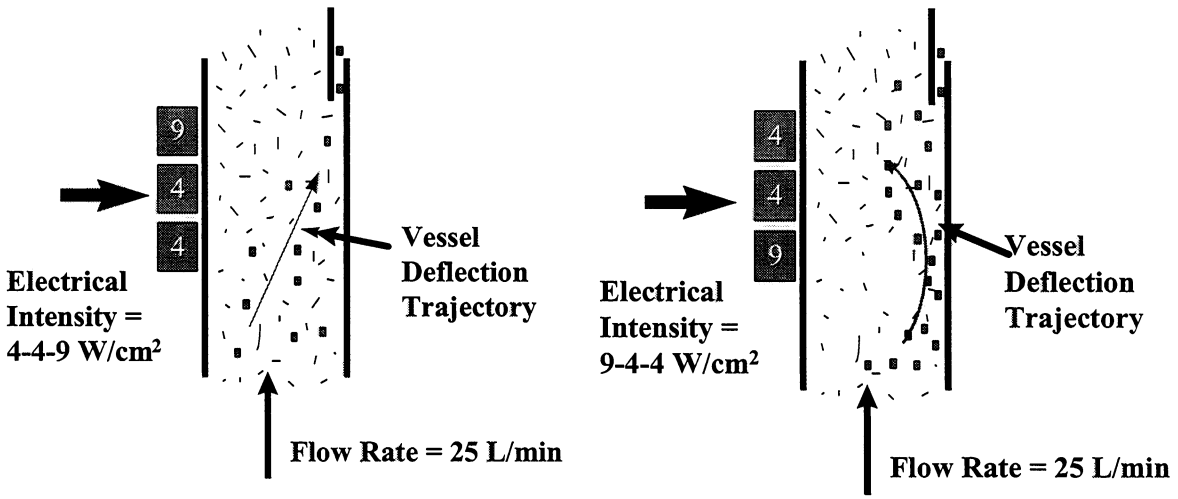

Figure 17. Acoustic trajectories for the two different transducer configurations. Figure on left is for experiment C, Figure on right is for experiments A, B and D.

It is clear that the above results are less than satisfactory. Nevertheless, they indicate that acoustic radiation pressure has an effect on large vessels.

Another series of experiments was performed in November 1997 using Eucalyptus and Oak furnishes. While every attempt was made to maintain similar test conditions in order to reproduce results previously obtained using Eucalyptus pulp, data analysis was performed by another person. Measurements were found to be marginal. More importantly, they confirmed that the vessel counting method was seriously deficient and prevented any optimization work about acoustic separation. Not until a rapid and reliable test method is available that a comprehensive study of acoustic separation of vessels and hardwood fibers can be performed (see Section 6).

There are numerous test conditions waiting to be investigated: flow rate, acoustic cell width, mechanical divider location, acoustic dwell time, acoustic intensity, frequency, pulp consistency. Also, in addition to a traveling wave field configuration, experiments using a stationary ultrasonic wave field must be conducted for at least two reasons: 1) at equal power level, the acoustic force in a stationary ultrasonic wave field can be three to four orders of magnitude larger, thus enabling separation at significantly lower power levels; 2) the migration distance for vessels is significantly less (few millimeters between agglomeration planes instead of centimeters between transducer and absorber positions), thus increasing vessel separation efficiency.

6. Automated Detection of Vessels in Hardwood Furnish (Brian Pufahl)

Due to the subjectivity and length of time associated with manually inspecting fiber samples, it was decided to initiate the development of an automated image analysis system for vessel detection. The system differs from traditional fiber inspection in that it relies on a high-resolution digital camera with standard lenses rather than microscopy. By utilizing the high-resolution camera, it is possible to analyze much larger sample areas than microscopy while maintaining the resolution necessary to distinguish vessels from other components in the sample. In addition, the sample is mounted on a motorized X-Y table which allows the use of 6"x6" slides in place of the typical 1.5"x1" microscope slide. Figure 18 shows a schematic diagram of the camera-based system.

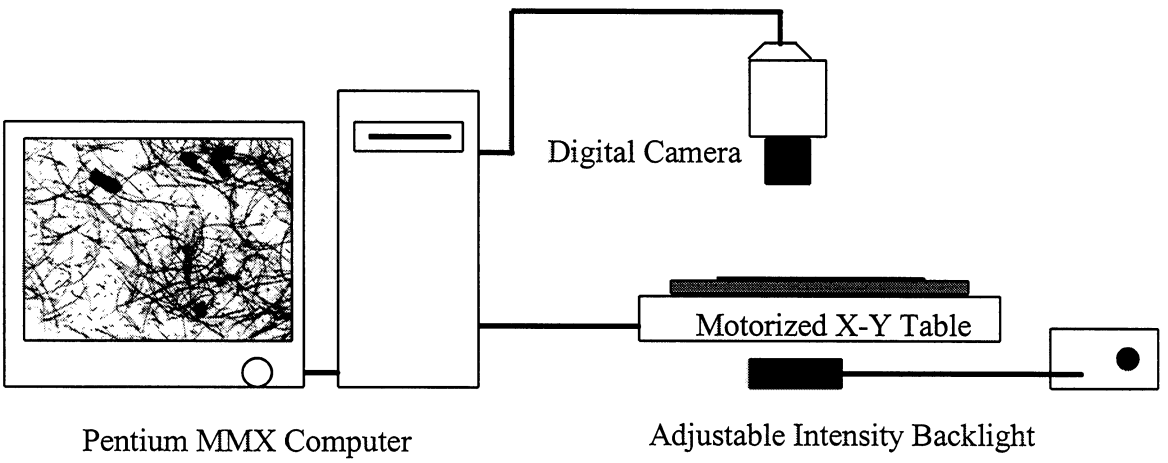

Figure 18. Schematic of Image Analysis System used for vessel detection in microscopy slides.

All features of the system including sample positioning and image acquisition are controlled by a Pentium MMX personal computer running under Windows 95. Although commercial image analysis products could be applied to this system, these programs

are not capable of providing system control and would require highly trained operators. For these reasons, a custom programmed LabView-based software package is utilized to provide system control, image analysis, report generation, and data archival. This software provides a graphical operator interface and allows samples to be processed with a minimal amount of operator training or input. Outputs from the software will include total number of vessels and vessel size distribution.

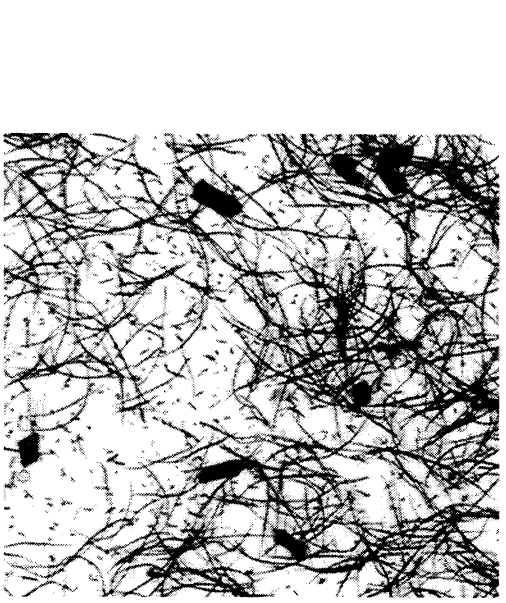

Partial Image from Digital Camera

Full Image from Microscopy

Figure 19. Comparison of imaging systems.

Figure 19 contains images taken with the digital system compared to traditional microscopy. Although the resolution of the systems are comparable in these images, the digital system provides a wider dynamic range and a much larger viewing area. In the figure, the digital image has been cropped from 1528x1023 pixels to 500x500 pixels (approximately 1/6 of the total picture) while the microscopy image is presented at its

full size of 480x640 pixels. Although not apparent in the raw image, the analog camera also contains a slight "halo" effect due to the distribution of lighting in the microscope system.

In conjunction with the development of the automated digital imaging system, new fiber staining techniques are being investigated (David Rothbard and Blair Staley, IPST Microscopy Group). These techniques are required to reduce slide preparation time, enhance contrast between vessels and fibers, and provide a stain which will not change over time. Previously, "C-stain" was used as the staining agent but had three major drawbacks: it did not provide sufficient contrast between the fibers and vessels, it stained different fiber species in different ways, and it would continue to darken over time. Recent trials with "Victoria B" and "Safranin" stains suggest that short term exposures to these stains provide good contrast between the vessels and fibers along with a permanent "set". These trials continue with the adjusting of stain concentration, exposure time, and possible combination of the two stains.

7. Literature Cited

[1] Brodeur, P.H., "Motion of Fluid Suspended Fibers in a Standing Wave Field," *Ultrasonics* 29:302-307 (1991).

[2] Brodeur, P., Dion, J.L., Garceau, J.J., Pelletier, G., and Massicotte, D., "Fiber Characterization in a Stationary Ultrasonic Field," *IEEE Trans. Ultrason. Ferroelec. Freq. Control.* 36:549-553 (1989).

[3] Garceau, J.J., Dion, J.L., Brodeur, P., and Luo, H., "Acousto-optical Fiber Characterization," *Tappi J.* 72:171-173 (1989).

[4] Dion, J.L., Brodeur, P., Garceau, J.J., and Chen, R., "Caractérisation des fibres par un nouveau procédé acousto-optique: nouveaux résultats." *J. Pulp & Paper Sci.* 14:J125-J128 (1988).

[5] Brodeur, P.H., "Acoustic Separation in a Laminar Flow," Proc. IEEE Ultrasonics Symp., Cannes, France Vol. 3:1359-1362 (1994).

[6] Brodeur, P.H. and Runge, T.M., "Compactibility of a Wet Fiber Mat Using Acoustic Radiation Pressure," *J. Pulp & Paper Sci.* 22(8):J278-J282 (1996).
[7] Oakland, M.O., "Separation of Vessel Elements from Hardwood Fibers Using an Ultrasonic Method," M.S. Research Report, IPST (1997).
[8] Blanz, "The Application of Acoustic Cavitation Towards Refining of Cellulose Fibers," M.S. Research Report, IPST (1997).
[9] Awagani, J. "Study on Acoustic Radiation Pressure (IV) (Radiation Pressure on a Cylinder," Memo. Inst. Sci. Ind. Research Osaka Univ. 12:95-102 (1955).
[10] Zhuk, A.P., "Radiation Force Acting on a Cylindrical Particle in a Sound Field" Soviet Appl. Mech. 22(7):689-693 (1986).
[11] Hasegawa, T., Saka, K. Inoue, N., and Matsuzawa, K., "Acoustic Radiation Force Experienced by a Solid Cylinder in a Plane Progressive Field," J. Acoust. Soc. Am. 83(5):1770-1775 (1988).

FUNDAMENTALS OF DIMENSIONAL STABILITY

STATUS REPORT

FOR

PROJECT F020

Douglas Coffin
Barry Hojjatie
Kennisha Collins
Frederick Bloom

Institute of Paper Science and Technology
500 10th Street, N. W.
Atlanta, Georgia 30318

DUES-FUNDED PROJECT SUMMARY

Project Title: Dimensional Stability

Project Code: DIMSTAB

Project Number: F020

PAC: Paper Physics

Division: Fiber and Paper Physics

Project Staff: PI: Douglas Coffin

Staff: Barry Hojjatie, Kennisha Collins, Frederick Bloom

FY 97-98 Budget: $110,430

Time Allocation: Faculty: 25%, Staff: 60%

Supporting Research: MS Student: Michelyn Rae McNeal (MS 99): Paper Curl

RESEARCH LINE/ROADMAP:

11 *Convertibility and End-Use Performance*

Improve the ratio of product performance to cost for pulp and paper products 25% by developing: models, algorithms and functional samples of fibrous structures and coatings which describe and demonstrate improved convertibility and end-use performance.

PROJECT OBJECTIVE:

Reduce the amount of paper rejected because of cockle through improved efficiency in identifying the causes of cockle and/or use of corrective measures to prevent cockle.

To develop a science-based understanding of the dimensional stability of paper and paperboard, especially the phenomenon of cockle, and to apply these fundamental results to practical industrial problems.

PROJECT BACKGROUND

This project was initiated and started in July of 1994. The scope of work for this project is to gain an understanding of cockle in paper and to develop the knowledge and tools required to eliminate its occurrence. Cockle is a manifestation of the dimensional instability of paper due to local variations in the physical state of the paper coupled with a change in moisture content. The phenomenon of cockle is directly related to the mechanical, hygroexpansive, and physical properties of paper. These properties will be a result of the constituent materials and the papermaking process used to produce the sheet. With an understanding of how cockle occurs, steps can be taken to eliminate it by modifying the constituent materials or papermaking process. Since cockle is inherently a complex problem and is influenced by many different factors, the advances made in this research program will benefit the scientific understanding in all areas of dimensional stability.

SUMMARY OF RESULTS (March 97-March 98)

- New Tools Developed
  - Humidity Chamber: Completed construction for tests such as hygrobuckling and moisture sorption studies.
  - Hygroexpansive Buckling Tester: Completed construction of testing apparatus for producing buckling of paper strips resulting from an increase in moisture.
  - Shadow Moiré Topography System: Designed in conjunction with Electronic Packaging Services at GTRI. Used to quantify cockle and curl.

- Testing Completed

  -Hygrobuckling: Developed testing procedures. Measured postbuckling response of several paper types. Developed a method to determine an effective hygroexpansion coefficient for paper.

-Cockle Measurements: Using the Shadow Moiré system measured topography of cockled samples of paper. Changes in cockle with cyclic humidity studied.

•Other Activities

- Developed a survey form from which we hope to gain better insight into the important characteristics of cockle.
- Developed algorithms to calculate curvature from Shadow Moiré results.
- Completed member company reports 3 and 4 which constitute an in-depth survey of general buckling [2] and thermalbuckling [3] of thin plates.

PROJECT GOALS FOR FY 98-99

- Conduct survey of printers.
- Conduct investigation of cockle as a function of process variables and cyclic humidity for handsheet study.
- Conduct hygrobuckling experiments for copy paper.
- Develop numerical simulation of cockle.

PROJECT DELIVERABLES: Reports for printer survey, handsheet study, hygrobuckling study.

PROJECT SCHEDULE

TASK		98a	98b	99a	99b	00
Hyygro-buckling	strip buckling tests	------	–			
	numerical model	------	------	-------		
	sheet buckling tests		------	-------	-------	
Cockle Tests	sensitivity studies	------	------			
	specific studies			-------	-------	-------
Cockle Evaluation	printer survey	------	–			
	cockle characterization	------	------	-------	-------	-------
	property correlation		----	-------	-------	-------
	cockle classification				-------	-------

DISCUSSION

The dimensional stability of paper is one of the primary concerns for many paper grades. The interaction between moisture and paper effects the entire life of paper from forming through converting to the end-use of the final product. Dimensional instabilities, such as curl and cockle, are blatant examples of the detrimental aspects of moisture and paper. Not so obvious are the loss of modulus or the accelerated creep caused by the interaction of moisture and paper. Thus, gains in the fundamental understanding of dimensional stability are essential to improving the efficiency of the papermaking process.

Cockle is one such area that has not been sufficiently addressed in a scientific manner yet is prevalent in the paper industry. Thus, cockle was chosen as the focus of our excursion into dimensional instability. The plan for the current project was based on the following hypothesis for the cause of cockle.

> *Cockle results from an in-plane variation of the free hygroexpansive strains resulting from a change in moisture content of the sheet. The nonuniformity in the potential for free expansion creates compressive stresses in the sheet. If the compressive stresses are of sufficient magnitude, the sheet will buckle out-of-plane; thus, creating cockle. The free hygroexpansive strain is the stress free strain resulting from a change in dimensions of a material undergoing a change in moisture content. In addition to the nonuniformity in the free hygroexpansive strains, planar nonuniformities in mechanical or physical properties must be present to induce local buckling of the sheet.*

In trying to get to our destination, minimizing cockle, we have set out on three different roadways. Along each roadway we hope to gather sufficient evidence such

that at the end of our path we clearly see that we have arrived. The three roadways all head in the same direction and intersect each other along the way.

First, we are saying cockle is a buckling phenomenon and are studying the theory of plate buckling. Second, we are saying that buckling arises from the restrained expansion/shrinkage of the sheet and are investigating hygrobuckling of a sheet. Third, we are saying that cockling arises from planar variations in properties arising from variability introduced in papermaking, thus we are studying the effects of variability and process conditions on the severity of cockle. The following highlights our foward progress made in the last year on each of these avenues of research.

Buckling and Postbuckling Theory

We are now in the process of formulating a model that will predict the buckling of sheets due to changes in moisture content. The model will account for planar variations in thickness, mechanical properties, and moisture histories; as well as two-sidedness. Imperfections in the original flatness of the sheet will be accounted for. Initially, we will treat the sheet as a thin elastic material but may need to account for inelastic effects. We will assume that the material properties are orthotropic but may vary from location to location in the sheet. For this idealized material, which we hope captures the essence of paper, we will predict the deformed geometry of the sheet when it is subjected to a change in moisture content. In other words, we will try to simulate cockle.

It is probably not possible to predict the exact buckled shape for a specific piece of paper, but we expect to predict the general trends of cockle as a function of the type and degree of variability. Thus, the model can be used as a tool to study sensitivities and determine the most likely causes of cockle.

During the last fiscal year we issued a member company report that summarized our critical review of the literature [1]. The full report from which we summarized the results was issued as a member company report this year [2]. It gives a detailed account of how to conduct a buckling and postbuckling analysis of thin plates. The effects of parameters such as material symmetry, geometry, inelasticity, and imperfections were reviewed. By using the summary given in reference [1], one can interpret the type of buckled pattern that they observe in their paper. This insight may help determine a method to eliminate the problem.

In the review [1,2], we concentrated on buckling due to applied compressive thrusts. There is also rich literature in the area of thermal buckling. Our review of this literature was issued as member company report number 4 [3]. This report is available to member companies upon request.

From a mathematical viewpoint, swelling due to moisture change is the same as thermal expansion. Therefore, we can apply the results from report number 4 [3] directly to our study on cockle in paper. In reviewing this literature on thermal buckling, we found several analyses that contained errors. These questionable results are discussed in the report, and create an opportunity for some original work of interest to the scientific community.

The model that we are now in the process of formulating will be based on the knowledge we acquired from the literature search [1-3].

Hygroexpansive Buckling

Last year we discussed the buckling of a paper strip restrained from expansion and subjected to an increase in moisture content. As the moisture increases, the paper wants to swell, but it cannot. Compressive stresses are created and the sample buckles out of the plane of the sheet to relieve the stresses. This year we finished construction of our hygrobuckling tester. We have completed some preliminary testing as discussed below.

The hygrobuckling tester, shown as a schematic in Figure 1, will measure the axial load and the out-of-plane deflection of a test sample as the moisture level increases. In addition, the weight gain of a similar sample is measured. The buckling sample is in the form of a strip, up to 0.5 inches wide and 6 inches long. Both ends of the strip are clamped and restrained from any axial movement. The clamp on one side of the strip is connected to a load cell. The load cell will measure the axial load that is present in the sample. The out-of-plane deflection of the sample is measured with a laser displacement sensor.

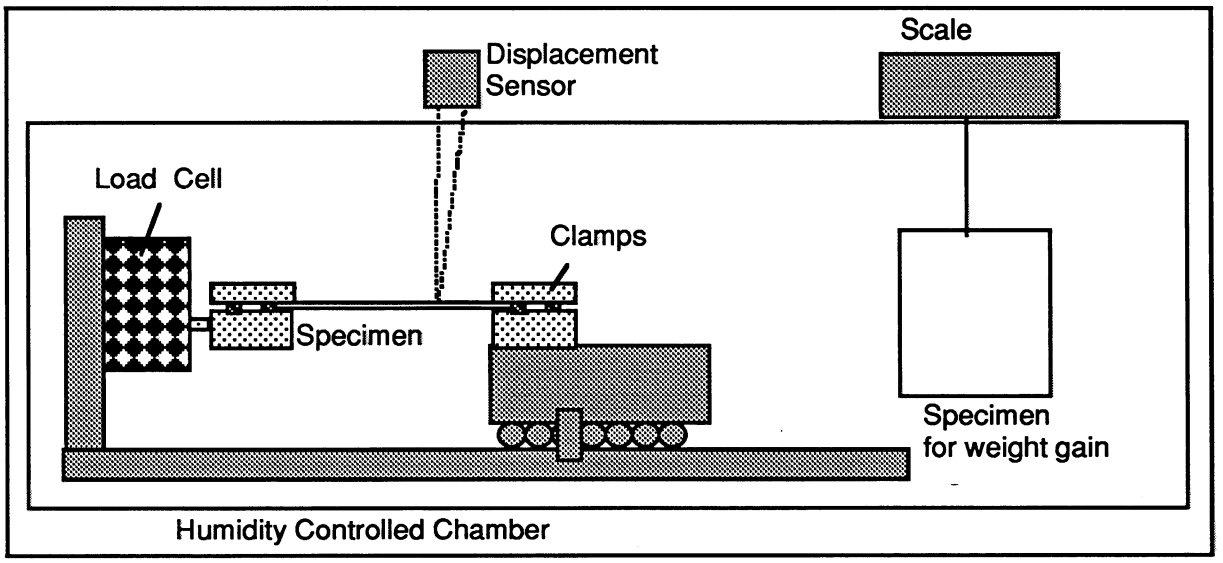

Figure 1. Hygrobuckling Tester.

Last year, we discussed the analytic solution which predicts the buckling and postbuckling response of the strip. The solution predicts that an initial period of moisture gain is accompanied by a compressive axial load, but zero deflection. At some critical increase in moisture content, the axial load will equal the critical buckling load of the strip. Any increase in moisture above this critical level will result in out-of-plane deflections (buckling) and a decrease in the axial load. If our strip is actually buckling, we will expect to observe this type of behavior.

The solution we obtained is in the form of two coupled integral equations. It was solved in the same spirit as Euler's original problem of the Elastica. Interestingly enough, the problem has not previously been solved, even for the thermal case. Thus, we are presently preparing this solution as a journal ariticle for the *International Journal of Nonlinear Mechanics*. The Paper Physics PAC approved this action at the Fall 1997 meeting.

Our solution is for the ideal case where everything is perfect. Of course, with paper we are far from perfection. Thus, we will expect to see small out-of-plane displacements before the critical load is reached, but the deflection should increase at a faster rate after buckling. In addition, we know the stiffness will decrease as the moisture increases. Thus, we expect to see the load drop faster in the experiments then our model would predict. We do expect that the critical buckling load would be the maximum load observed.

We have conducted tests on several paper grades including copier paper, medium, linerboard, and card stock. In general, we did see the results as expected. The load levels for the copier paper were quite low and the noise levels were too great for

accurate readings. If we continue with these tests, we will need a more sensitive load cell (available for $500.)

Figures 2 and 3 give results obtained with the hygrobuckling tester. These were determined for CD strips cut from an unbleached board grade with the following material properties: caliper=30 mils (0.764 mm), grammage=414 gsm, width=15.9 mm, length=50 to 150 mm. Note that the axial load increases substantially as moisture begins to diffuse into the sample. The load peaks and then drops off quickly. At the point where the load peaks, the deflection begins to increase. Thus, the experimental observations appear to correspond with our analytic results.

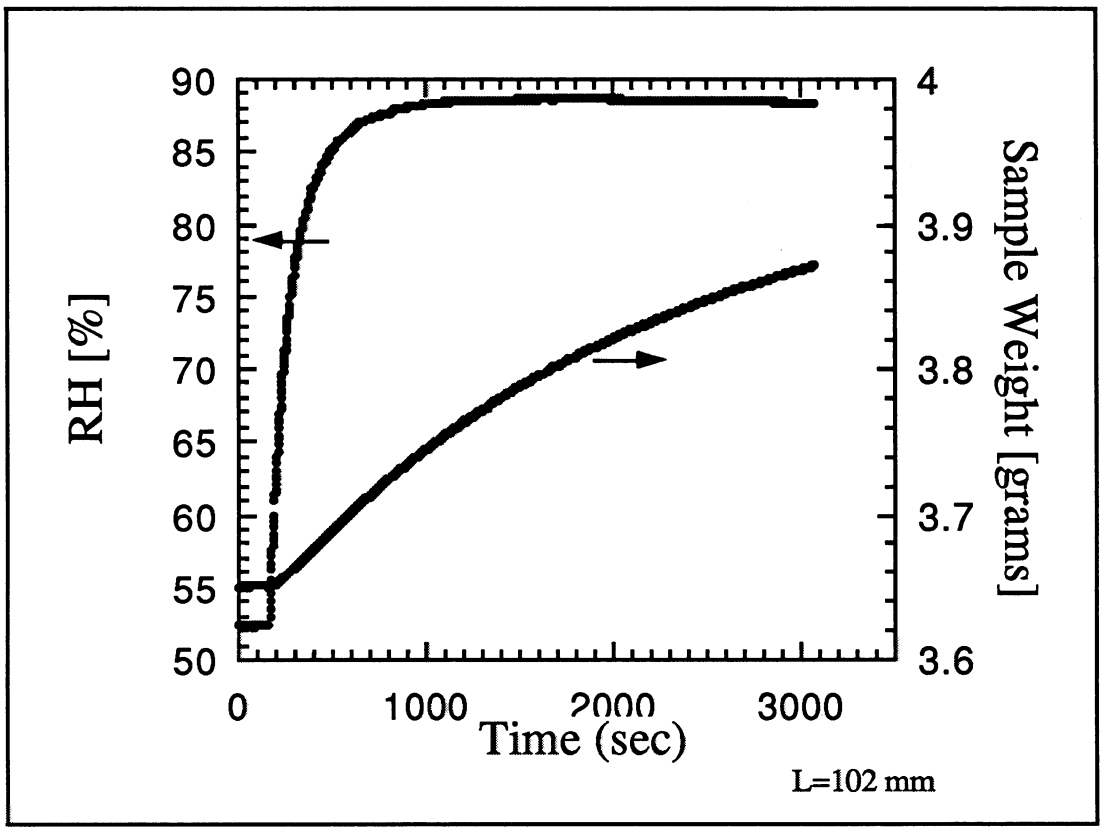

Figure 2. Relative humidity and moisture pickup versus time for hygrobuckling test.

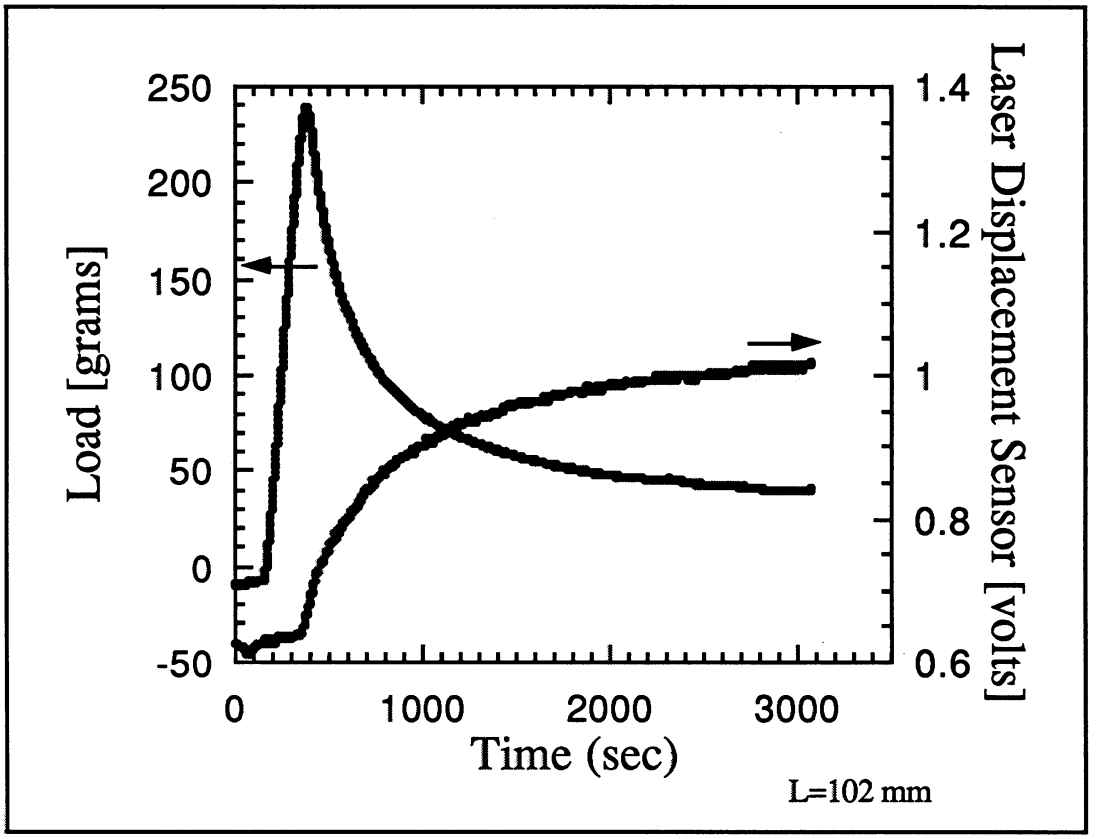

Figure 3. Axial Load and vertcal displacement versus time for hygrobuckling test.

Let us define the moisture content at the peak load as the critical moisture content which induces buckling and the peak load as the critical buckling load. According to our buckling theory, the critical moisture change should be proportional to the square of the ratio of the thickness to length (t/L). Figure 4 shows a plot of the critical moisture content versus $(t/L)^2$. Note, a fairly straight line can be fit through the data.

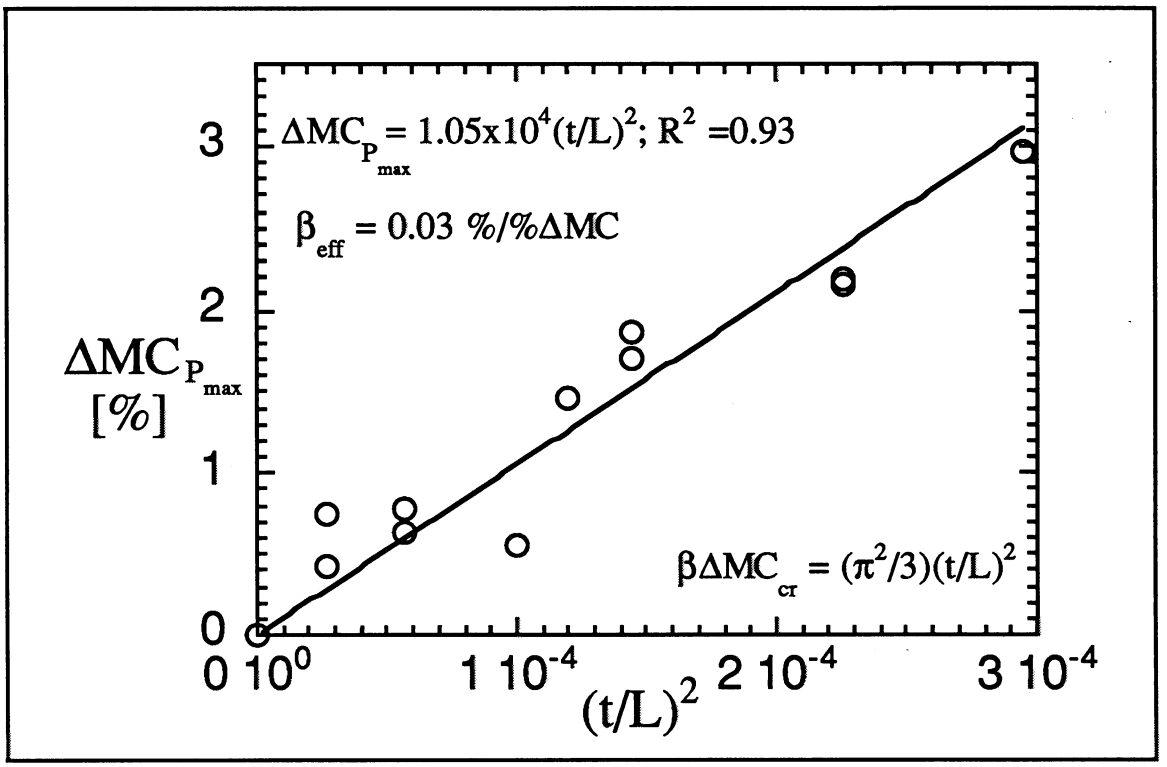

Figure 4. Moisuture pickup at peak load as a function of sample length.

The slope of the line shown in Figure 4 should be proportional to the coefficient of hygroexpansion. Thus, this test procedure may be a plausible method to calculate an effective coefficient of hygroexpansion for the sample. From the fit of the data given in Figure 6, we have calculated an effective coefficient of hygroexpansion of 0.03 %strain/%ΔMC. We measured a value of 0.09 %strain/%ΔMC in the Neenah hygroexpansivity cabinet. Thus, our test shows buckling at moisture levels three times lower than would be predicted. We need to verify this with repetitions. If the discrepancy holds true, we will need to investigate why this is so. It could be due to the fact that the bending stiffness to axial stiffness is not equal to $(t/L)^2/12$ as assumed in the model. This merits further investigation.

This hygobuckling tester, as far as I know, is unique. It may lead to new insight into moisture induced buckling, and hence cockle. If we can understand the mechanics

of the simple case of strip buckling, we will have a better idea of how to handle the complicated case of cockle.

Cockle Measurements

In last year's progress report, we alluded to the fact that we were looking to acquire a Shadow Moiré system for measuring full-field sheet topography. In fact, we did get just such a piece of equipment. We worked with Electronic Packaging Services (EPS, 430 10th Street, Atlanta, GA) to design a system that would measure sheet topography in a controlled-humidity environment. EPS produces Shadow Moiré systems for the electronics industry thay are used in applications such as checking flatness of printed circuit boards. Ours was the first unit of its type to be used in the lab for paper.

The system is designed to make noncontact field measurements of the distance from the surface of the sheet to a reference plane. This is accomplished by forming Moiré fringes of dark and light areas that follow surface contours of the sheet. Direct height measurements are obtained by taking three such fringe patterns where the distance between the sheet and reference plane are moved a known distance.

The fringes are formed by casting the shadow of a grating onto the sheet at an angle to the reference plane (36.5°) and viewing the shadow through the grating from above. The shadows and the lines interfere with each other forming contours that pertain to a known change in height. Our unit is set up for a Ronchi rule grating with 50 lines per inch or 100 lines per inch. For one fringe pattern, this gives us a height resolution of either 13.5 mils for the 100 lines per inch and 27 mils for the 50 lines per inch. By itself this resolution is not adequate, but by phase stepping the distance

between the sample and reference plane we can improve our resolutions to 1.5 and 3 mils, respectively.

Three phase steps are completed by stepping the distance at a third of the resolution. The three fringe images are combined in such a way that detailed height and gradient information are obtained.

The images are captured with a video camera, a frame grabber and a PC. The final output of the system is a height for each pixel of the image. This gives the full-field topography of the sample. The reference plane can be taken as either the plane of the glass plate, the plane fit through three corners of the image or the best fit plane of the data. For cockle measurements, we usually choose the best fit plane. This gives a mean height of zero.

We have used the instrument to measure cockle for a series of machine-made copier papers. We were able to quantify the cockle numerically, but the task to determine the best quantities in which to quantify the severity of cockle remains unsolved. For the set of sheets, we rated the cockle according to visual severity on a scale of 1 to 5. Most of the sheets were rated as a 2 or a 4. The 2's were fairly flat sheets with very slight cockle. The 4's had many small cockles. We compared the standard deviation of the sheet heights to the cockle rating. The average of the standard deviations in height for the number 2 sheets was 2.7 mils (0.4 mils. std.dev.) and for the number 4 sheet we found a value of 3.6 mils (0.7 mils std. dev.). In general, the measurements showed that sheets we perceived as having more severe cockle did have a higher variation in surface topography, although the variation in our data is quite large. We need to further investigate cockle parameters.

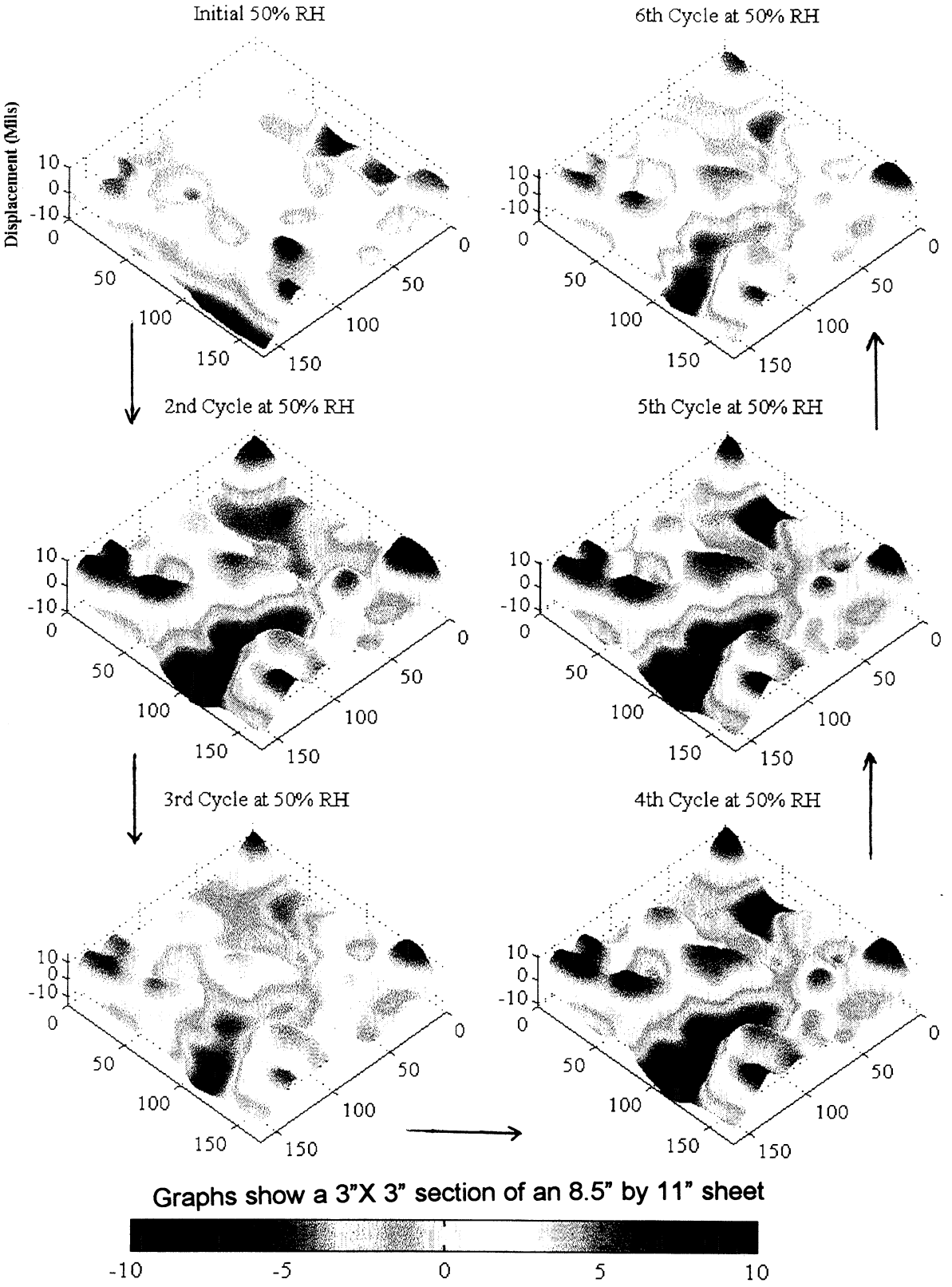

Figure 5. Effect of cyclic humidity on sheet topography. Figure shows sheet height at initital 50% RH and at 50% RH after excursions to 85% RH

A unique feature of our system is that we can observe differences in cockle due to changes in moisture. The sample is placed in a humidity-controlled chamber. We can take fringe images at any time and calculate topographies at different equilibrium states. In terms of understanding our mechanism, we are interested in how cockles vary with changes in moisture. To measure this change, we took one of our cockled sheets and cycled the humidity from 50% RH to 85% RH six times. Each time the sample was at 50% RH, we calculated the topography of the sheet. We also determined the topography the first time the sheet was at 85% RH and the last time it was at the high RH (actually 80 % RH for last step). Figure 5 shows the sequence of topography maps at the 50% RH level. It is clear that the severity of cockle increased dramatically after the first cycle with only slight changes in subsequent cycles. Interestingly, we found that when the sheet was increased to 85% RH for the first time the cockle heights changed very little, but substantially increased during the decrease back to 50 % RH. These results indicate that most of the cockle change could be a result of releasing "dried-in strains." The height of cockles at the final 80% RH level is much lower than the 50% RH heights. Table 1 provides maximum, minimum, and standard deviations for the heights at the different time intervals.

Table 1. Summary of height data for effect of cyclic humidity on cockle.

Cycle Time	Max. Height (mils)	Min. Height (mils)	St. Deviation (mils)
inital 50 % RH	7.8	-8.7	2.5
first 85%	8.7	-6.7	2.7
2nd 50% RH	10.8	-10.7	4.1
3rd 50% RH	12.6	-9.7	3.9
4th 50 % RH	11.6	-11.1	4.3
5th 50 % RH	11.1	-13.0	4.6
6th 50 % RH	12.1	-10.0	4.0
6th 80 % RH	8.2	-7.6	3.3

These results suggest that some thought may be warranted on developing methods to minimize cockle growth in a cyclic humidity environment, and we may be able to develop methods that eliminate cockle.

Future Plans

During the last year, we have developed several useful testing techniques to help in our journey to eliminate cockle. Our review of buckling theory and development of several solutions has helped us focus our efforts in the right direction. The hygrobuckling apparatus may lead to new insights that will guide us in planning cockle tests and in developing the numerical simulations of cockle. The development of the Shadow Moiré system has opened the door to characterizing cockle in a reliable and efficient way.

We would like to continue using the hygrobuckling apparatus to characterize moisture-induced buckling of paper. We would like to compare our experimental results to a numerical solution that predicts the postbuckling behavior. If we can

achieve this goal, we will have confidence that we understand the important sheet properties governing this phenomenon. We hope that in the future this apparatus will be useful for characterizing the behavior of paper.

We are ready to conduct an experimental study of cockle in handsheets. We plan to make a set of handsheets where we vary certain parameters such as furnish, freeness, basis weight, density, drying restraint, and rates of drying. Then, we will evaluate the flatness of the dried sheet and changes in flatness during cyclic humidity testing. The results of these tests will provide correlation of cockle severity to the process conditions. This information will prove useful to help evaluate cockle in machine-made papers.

Finally, we still need to develop the appropriate topographical parameters for analyzing the severity of cockle. We plan on conducting our survey of printers in the hopes of finding out what they perceive as good and bad paper. We will try to turn the printer's perception into parameters that can be calculated from the topography data. This will be accomplished by pulling together everything we have learned and hope to learn.

References

1. D. W. Coffin and F. Bloom, *Cockle and Hygroexpansive Buckling: A Survey of Initial Buckling and Postbuckling of Thin Plates*, Project E00102, Report 1 to the member companies of the Institute of Paper Science and Technology, September 1996.

2. D. W. Coffin and F. Bloom, *A Critical Review of the Analysis of Initial Buckling and PostBuckling of Thin Plates*, Project E00102/F020, Report 3 to the member companies of the Institute of Paper Science and Technology, March 1997.

3. F. Bloom and D. W. Coffin, Hygrothermal Buckling and Bending of Thin Plates, Project F020, Report 4 to the member companies of the Institute of Paper Science and Technology, February 1998.